ISSN : 0019-5693

INDIAN JOURNAL
OF
THEORETICAL PHYSICS

VOLUME 65 NOS. 1, 2

JANUARY, 2017 — JUNE, 2017

Published by the
CALCUTTA INSTITUTE OF THEORETICAL PHYSICS
(Formerly, INSTITUTE OF THEORETICAL PHYSICS)
"BIGNAN KUTIR"
4/1, MOHAN BAGAN LANE, KOLKATA-700 004

(UGC approved and refereed Journal)

ISSN : 0019-5693

INDIAN JOURNAL
OF
THEORETICAL PHYSICS

VOLUME 65 **NOS. 1, 2**

JANUARY, 2017 — JUNE, 2017

Published by the

CALCUTTA INSTITUTE OF THEORETICAL PHYSICS
(Formerly, INSTITUTE OF THEORETICAL PHYSICS)
"BIGNAN KUTIR"
4/1, MOHAN BAGAN LANE, KOLKATA-700 004

(UGC approved and refereed Journal)

ISSN : 0019-5693

INDIAN JOURNAL
OF
THEORETICAL PHYSICS

[Founder President : Late Prof. K. C. Kar, D.Sc.]

VOLUME 65 **NOS. 1 2**

JANUARY, 2017 — JUNE, 2017

Co-Published by the

WILCOX BOOKS & PERIODICALS CO.

8/2/A, Neogipara Road, Kolkata – 700 036

BLANK

INDIAN JOURNAL
OF
THEORETICAL PHYSICS

"BIGNAN KUTIR"
4/1, MOHAN BAGAN LANE, KOLKATA-700 004, INDIA

SUBSCRIPTION RATE

INDIA : (For Library & Institute)
₹ 1500.00 for Vol. 64, 2016 and onwards
FOREIGN : $ 350 for Vol. 64, 2016 and onwards
Drafts, Orders, Enquiries & Claim for Non-Receipt of Journal should be sent to :

WILCOX BOOKS & PERIODICALS CO.
8/2/A, NEOGIPARA ROAD
KOLKATA – 700 036 (INDIA)
Website : www.wilcoxjournals.com
E-mail : wilcoxbooks@yahoo.com
: wilcoxbooks@gmail.com
Phone : 91-3325771147
Mobile : 91-9231675520

BLANK

C O N T E N T S

BLANK

INDIAN JOURNAL OF THEORETICAL PHYSICS, VOL. 65, NOS. 1 & 2, 2017

Evaluation of activation energy in thermoluminescence recorded under linear heating profile

SK. Azharuddin*, B. Ghosh
Department of Physics, Jadavpur University,
Kolkata-700 032, India

and

S. Dorendrajit Singh
Department of Physics, Mainipur University
Canchipur, Imphal-795003

(Received for publication in January, 2017)

[**Abstract :** Peak shape method has been used to determine the activation energy of a *TL* peak. In conventional peak shape method only the half intensity points are used. In the present paper peak shape formulas has been developed by using points with fractional intensities 2/3 and 4/5. This has been done to reduce the error due to overlapping from satellite peaks. Finally the formulaes have been applied to experimental peaks of Sodalite.]

Key words : Peak shape method (PSM), order of kinetics, symmetry factor, activation energy.

1. Introduction

Thermally Stimulated Luminescence (*TSL*) or Thermoluminescence (*TL*) is the light emission that occurs when heat is applied to an insulator or a semiconductor which has been previously irradiated by ionizing radiation[1, 2]. The intensity of emitted *TL* may vary although it is generally very weak. However in very rare occasion the intensity is high enough to be seen by the naked eye. Of course the irradiation depends on the material and the quality of previously absorbed radiation. *TL* occurs in both insulator and semiconductors. A forbidden gap in the band structure of a material is necessary to allow for localized levels, associated with defects, to be present in the material. As a result conductors do not exhibit *TL*. Most of the literature related to *TL* deals with insulating materials. Due to this fact in practice *TL* is studied in insulators, mostly in which traps are deep enough

*Communicating Author : SK. Azharuddin, E-mail : az2har3@rediffmail.com

to be stable at room temperature and so that light is emitted in the visible region. Usually *TL* is studied by using linear heating scheme and is described by three parameters namely order of kinetics (b), frequency factor (s) and activation energy (E). Activation energy is the most important trapping parameter because life time of a trap which is crucial for dosimetric and dating purposes depends on E. Peak shape method (*PSM*) is one of the simplest methods[1, 2] of determination of activation energy. Normally in peak shape method half intensity points are used but Fleming[3] suggested the possibility of using points in upper portion of the peak corresponding to the fractional intensity x ($x = I / I_m = 2/3$ and 4/5, $I =$ intensity corresponding to any point of *TL* curve, $I_m =$ peak intensity). In practice the activation energy as calculated by *PSM* by using half intensity points might be affected by interference from other satellite peaks. So it is better to calculate the activation energy corresponding to points in the upper half of a *TL* peak such as $x =$ 2/3 and 4/5. Usually upper half of a *TL* peak is not affected much by interference from satellite peaks. Singh et. al.[4] suggested a relation between symmetry factor (μ_g)[1, 2] corresponding to $x = 1/2$ and order of kinetics (b) for the determination of order of kinetics. But they limited their studies to half intensity points ($x =$ 1/2). In the present paper we apply the peak shape method to the points in the upper half portion ($x = 2/3, 4/5$) of *TL* curve. Calculations also have been made for $\mu_g(x)$ (where $x =$ 2/3 and 4/5) as a function of b for linear heating scheme. Finally we have tested the applicability of our analysis by considering numerically computerized peaks and experimental *TL* peaks of Sodalite.[5]

2. Theory

The basic equation of *TL* in general order kinetics model is[6]

$$I = -\frac{dn}{dt} = s\frac{n^b}{N^{b-1}} \exp\left(-\frac{E}{kT}\right) \qquad \ldots \quad (1)$$

where E is the activation energy, T is the temperature at time t, n is the concentration of electrons in electron traps at time t. N is the concentration of electron traps, k is the Boltzmann constant, I is the *TL* intensity, s is the frequency factor, b is the order of kinetics.

The linear heating scheme can be represented as[1, 2]

$$T = T_0 + \beta t \qquad \ldots \quad (2)$$

T_0 is the initial temperature and β is the constant heating rate. Using equations (1) and (2) the *TL* intensity for general order kinetics (*GOK*) model can be expressed as

$$I = sNf^b \exp\left(-\frac{E}{kT}\right)\left[1+(b-1)s\frac{f^{b-1}}{\beta}\int_{T_0}^{T}\exp\left(-\frac{E}{kT'}\right)dT'\right]^{-\frac{b}{b-1}} \qquad \ldots \quad (3)$$

$f = n_0 / N$ is the filling ratio. For an unsaturated *TL* peak $0 < f < 1$, $f = 1$ represents a saturated *TL* peak. For $b = 2$ the equation reduces to expression for I reported by Garlick and Gibson[7] for second order kinetics (*SOK*). For $b \to 1$ using the well known limit[8]

$$\lim_{x\to 0}(1+x)^{\frac{1}{x}} = e \qquad \ldots \quad (4)$$

The expression for I corresponding to eqation (1) reduces to expression for I reported by Randal and Wilkins[9] for first order kinetics is given by

$$I = sn_0 \exp\left(-\frac{E}{kT}\right)\exp\left[-\frac{s}{\beta}\int_{T_0}^{T}\exp\left(-\frac{E}{kT'}\right)dT'\right] \qquad \ldots \quad (5)$$

The condition for maximum intensity for *GOK* model is given by

$$1+(b-1)f^{b-1}\frac{s}{\beta}\int_{T_0}^{T_m}\exp\left(-\frac{E}{kT'}\right)dT' = \frac{bskT_m^2}{\beta E}f^{b-1}\exp\left(-\frac{E}{kT}\right) \qquad \ldots \quad (6)$$

For b =1 the maximum intensity condition is given by

$$\frac{\beta E}{kT_m^2} = s\exp\left(-\frac{E}{kT_m}\right) \qquad \ldots \quad (7)$$

Now eliminating $\frac{s}{\beta}$ between equation (3) and equation (6) we get for $b \neq 1$ (non-first order kinetics)

$$\frac{I}{I_m} = \exp(u_m - u)\left[1-\frac{b-1}{b}F(u,u_m)\right]^{-\frac{b}{b-1}} (b \neq 1) \qquad \ldots \quad (8)$$

where $u = \frac{E}{kT}$ and $u_m = \frac{E}{kT_m}$, T_m is the peak temperature and I_m is the peak intensity.

Similarly elimination of $\frac{s}{\beta}$ between equations (5) and (7) for first order kinetics (b = 1) leads to the equation

$$\frac{I}{I_m} = \exp\left[u_m - u + F(u, u_m)\right] \quad \ldots \quad (9)$$

In both the equations (7) and (8) $F(u, u_m)$ is given by

$$F(u, u_m) = u_m^2 \exp(u_m)\left[\frac{E_2(u_m)}{u_m} - \frac{E_2(u)}{u}\right] \quad \ldots \quad (10)$$

$E_2(u)$ is the second exponential integral[10]. It can be expressed as[10]

$$E_2(u) = u\int_u^{\infty} \frac{\exp(-z)}{z^2}\, dz \quad \ldots \quad (11)$$

Using equations (9) and (10) by some suitable iterative method it is possible to find out temperatures in the *TL* peak for which $\frac{I}{I_m} = x$.

Let T_x be he temperature for which the fractional intensity $\frac{I}{I_m} = x$. For a particular value of x there will be two values of the T_x one for rising side of the peak and another for falling side of the peak. For clarity we write $T_x = T_x^-$ for $T_x < T_m$ and $T_x = T_x^+$ for $T_x > T_m$.

To a very good approximation a linear relation has been observed between the following pairs of variables

(i) u_m and $\frac{u_x^-}{(u_x^- - u_m)}$

(ii) u_m and $\dfrac{u_x^+}{(u_m - u_x^+)}$

(iii) u_m and $\dfrac{u_x^+ u_x^-}{u_m(u_x^- - u_x^+)}$

So that it is possible to write

$$u_m = A_{\tau_x} \frac{u_x^-}{(u_x^- - u_m)} + B_{\tau_x} \quad \ldots \quad (12)$$

$$u_m = A_{\delta_x} \frac{u_x^+}{(u_m - u_x^+)} + B_{\delta_x} \quad \ldots \quad (13)$$

$$u_m = A_{\omega_x} \frac{u_x^+ u_x^-}{u_m(u_x^- - u_x^+)} + B_{\omega_x} \quad \ldots \quad (14)$$

with $u_x^{\pm} = \dfrac{E}{kT_x^{\pm}}$

Finally equations (12)-(14) can be expressed as

$$E_{\tau_x} = A_{\tau_x} \frac{kT_m^2}{\tau_x} + B_{\tau_x} kT_m \quad \ldots \quad (15)$$

$$E_{\delta_x} = A_{\delta_x} \frac{kT_m^2}{\delta_x} + B_{\delta_x} kT_m \quad \ldots \quad (16)$$

$$E_{\omega_x} = A_{\omega_x} \frac{kT_m^2}{\omega_x} + B_{\omega_x} kT_m \quad \ldots \quad (17)$$

E_{τ_x}, E_{δ_x} and E_{ω_x} are respectively the activation energies corresponding to τ, δ and ω methods[1, 2]. For clarity a *TL* peak is shown in Fig 1. τ_x, ω_x and δ_x are respectively rising side half width, full width and falling side half width corresponding to the intensity ratio $\dfrac{I}{I_m} = x$ *i.e.*, $\left|T_m - T_x^-\right| = \tau_x$, $\left|T_x^+ - T_x^-\right| = \omega_x$ and $\left|T_x^+ - T_m\right| = \delta_x$.

In the literature[1,2] the value x = 1/2 is used for peak shape method[1,2,4,11]. E values as determined by using τ_x, ω_x and δ_x are denoted by E_{τ_x}, E_{δ_x} and E_{ω_x}

3. Results and discussion

The coefficients A_{ix} and B_{ix} in equations (15) to (17) can be expressed as a quadratic function of order of kinetics b

$$A_{ix} = A_{ix}^{(0)} + A_{ix}^{(1)} b + A_{ix}^{(2)} b^2 \quad \ldots \quad (18)$$

$$B_{ix} = B_{ix}^{(0)} + B_{ix}^{(1)} b + B_{ix}^{(2)} b^2 \quad \ldots \quad (19)$$

The coefficients $A_{ix}^{(0)}, A_{ix}^{(1)}, A_{ix}^{(2)}, B_{ix}^{(0)}, B_{ix}^{(1)}$ and $B_{ix}^{(2)}$ have been evaluated by using the technique of non-linear regression[12].The coefficients are presented in Table I for different values of fractional intensity (x). For clarity suffixes have been dropped from $A^{(i)}$ and $B^{(i)}$.

It is evident that in order to apply the relations corresponding to equations (15)-(17) to a particular *TL* peak (numerically computed or experimental) one should have prior knowledge of the value of order of kinetics (b), which can be obtained from the symmetry factor (μ_g) of *TL* peak. For arbitrary value of x the symmetry factor (μ_g) can be written as[6]

$$\mu_g(x) = \frac{T_x^+ - T_m}{T_x^+ - T_x^-} = \frac{(u_m - u_u^+)u_x^-}{(u_x^- - u_u^+)u_m} \quad \ldots \quad (20)$$

u_x^- and u_x^+ for a particular values of u_m, x and b can be obtained by solving equations (8) and (9) for $b \neq 1$ and $b = 1$ respectively by suitable iterative method[6].

Equation (20) shows that apart from b (equations (8) and (9)), $\mu_g(x)$ also depends on $u_m = \frac{E}{kT_m}$ for a particular value of *b*. Now for experimental *TL* peak E is unknown. As a result b cannot determined from μ_{g_x}. For

experimental *TL* peaks u_m is usually lies between 20 and 40[11]. Singh, et. al.[4] proposed a relation between $\mu_g(x)$ and b for $x = 1/2$ ($20 \le u_m \le 40$). This relation can be expressed as

$$\mu_g\left(\frac{1}{2}\right) = 0.245 + 0.186b - 0.024b^2 \quad \ldots \quad (21)$$

For $20 \le u_m \le 40$ $\mu_g(1/2)$ varies from 0.426 to 0.415 for b =1 and from 0.52 to 0.514 for b =2. So it is observed that the dependence of μ_g on b is much stronger than that on u_m. As a result equation (21) can be used for preliminary estimation of b. For $x = 2/3$ and $4/5$ the corresponding relations are given by

$$\mu_g\left(\frac{2}{3}\right) = 0.319 + 0.138b - 0.021b^2 \quad \ldots \quad (22)$$

$$\mu_g\left(\frac{4}{5}\right) = 0.361 + 0.103b - 0.016b^2 \quad \ldots \quad (23)$$

The values of b has been estimated for some computer generated *TL* peaks by using equations (21)-(23). Due to weak dependence μ_g on u_m, equations (21) to (23) leads to some error in the estimated values of b denoted by b_{est} in Table II.

Now the *PSM* formulas given by equations (15)-(17) have been applied to determine activation energies of some numerically computed *TL* peaks. The results are depicted in Table II show a fair agreement between calculated and input values of activation energy. It is to be noted that for the numerically computed peaks we have considerd the case $f = 1$ (fully saturated *TL* peaks) Encouraged by our findings for the case of numerically computed *TL* peaks we apply the peak shape formulas (equations (15) to (17)) to some experimental *TL* peaks of Sodalite which is one of the important rock forming minerals.

TL peaks of Sodalite irradiated with γ rays of dose 86 *KGy* (1 *Gy* is the deposit of one jule of radiation energy in a *Kg* of matter) recorded with heating rate of 1.67 ks^{-1} are isolated by thermal cleaning[5]. The individual peaks after thermal cleaning are presented in figures 2, 3 and 4. As per our findings in earlier sections the symmetry factor μ_{g_x} of the peaks are determined for fractional intensities 1/2, 2/3, 4/5. The order of kinetics of the peaks is estimated by using formulas in equation (21) to (23). The estimated values of order of kinetics indicate non first order kinetics for the peaks. For each peak the activation energies as determined by using points of different fractional intensities agree amongst themselves (Table III and IV) there by demonstrating the reliability of the values of activation energies.

Table I

Coefficients $A_{ix}^{(0)}$, $A_{ix}^{(1)}$, $A_{ix}^{(2)}$ and $B_{ix}^{(0)}$, $B_{ix}^{(1)}$, $B_{ix}^{(2)}$ occurring in equation (18) and (19) for $x = 1/2, 2/3$ and $4/5$.

x	i	$A_{ix}^{(0)}$	$A_{ix}^{(1)}$	$A_{ix}^{(2)}$	$B_{ix}^{(0)}$	$B_{ix}^{(1)}$	$B_{ix}^{(2)}$
1/2	τ	1.035	0.456	-0.047	-1.089	-1.145	0.083
	δ	0.119	0.884	-0.031	-0.205	-0.301	-0.955
	ω	1.151	1.338	-0.078	-0.887	-0.370	-0.533
2/3	τ	0.682	0.428	-0.051	-0.718	-1.19	0.095
	δ	0.147	0.687	-0.045	-0.181	-0.435	-0.092
	ω	0.828	1.111	-0.102	-0.524	-0.611	-0.028
4/5	τ	0.451	0.339	-0.045	-0.478	-1.187	0.087
	δ	0.154	0.491	-0.039	-0.182	-0.610	-0.063
	ω	0.603	0.832	-0.083	-0.295	-0.779	-0.005

Table II

Determination of order of kinetics and activation energy for computer generated *TL* peak E_{in} = 1.0 *eV*, $\beta = 1^{\circ}/s$, $f = 1.0$

s (sec^{-1})	x	b_{in}	T_m (K)	b_{cal}	E_τ (eV)	E_δ (eV)	E_ω (eV)
10(8)	0.5	1.0	536.48	1.1	1.02	1.09	1.05
		1.5	535.57	1.6	1.01	1.06	1.04
		2.0	534.71	2.0	1.00	1.01	1.01
	0.667	1.0	536.48	1.0	1.01	1.03	1.02
		1.5	535.57	1.6	1.02	1.05	1.03
		2.0	534.71	2.1	1.01	1.04	1.03
	0.8	1.0	536.48	1.0	1.03	1.07	1.05
		1.5	535.57	1.7	1.04	1.08	1.06
		2.0	534.71	2.3	1.04	1.08	1.06
10(12)	0.5	1.0	384.57	1.1	1.01	1.06	1.03
		1.5	384.21	1.6	1.01	1.03	1.02
		2.0	383.87	2.0	0.99	0.98	0.99
	0.667	1.0	384.57	1.0	1.00	1.00	1.00
		1.5	384.21	1.5	1.00	1.02	1.01
		2.0	383.87	2.0	1.00	1.02	1.01
	0.8	1.0	384.57	1.1	1.01	1.04	1.02
		1.5	384.21	1.6	1.02	1.05	1.04
		2.0	383.87	2.2	1.02	1.05	1.04

NB: *m(n)* denotes m^n

Table III

Activation energies of the *TL* peaks of Sodalite for different peaks.

Peak No.	T_m (K)	x	$\mu_g(x)$	b	s ($\sec^{-1}$)	E_τ (eV)	E_δ (eV)	E_ω (eV)	Mean E (eV)
1	383	0.5	0.538	2.2	1.47(7)	0.63	0.63	0.63	0.63
		0.667	0.500	1.8	1.51(7)	0.63	0.63	0.63	
		0.8	0.486	1.6	1.53(7)	0.63	0.63	0.63	
2	423	0.5	0.524	2.0	2.03(8)	0.79	0.79	0.79	0.79
		0.667	0.511	1.9	2.05(8)	0.79	0.79	0.79	
		0.8	0.486	1.6	2.09(8)	0.79	0.79	0.79	
3	510	0.5	0.500	1.8	1.21(11)	1.23	1.23	1.23	1.23
		0.667	0.511	1.9	1.20(11)	1.23	1.23	1.23	
		0.8	0.485	1.6	1.22(11)	1.23	1.23	1.23	

NB: $m(n)$ denotes m^n

Table IV

Standard deviation of the different values of order of kinetics and activation energy of experimental peak of Sodalite.

Peak No.	T_m (K)	b	$b \pm b_{SD}$	s ($\sec^{-1}$)	$s \pm s_{SD}$	$E \pm E_{SD}$
1	383	1.9	1.9 ± 0.23	1.503(7)	$1.50(7) \pm 0.02(7)$	0.63 ± 0.0007
2	423	1.8	1.8 ± 0.16	2.056(8)	$2.05(8) \pm 0.02(8)$	0.79 ± 0.0010
3	510	1.8	1.8 ± 0.11	1.21(11)	$1.21(11) \pm 0.008(11)$	1.23 ± 0.0016

NB: $m(n)$ denotes m^n

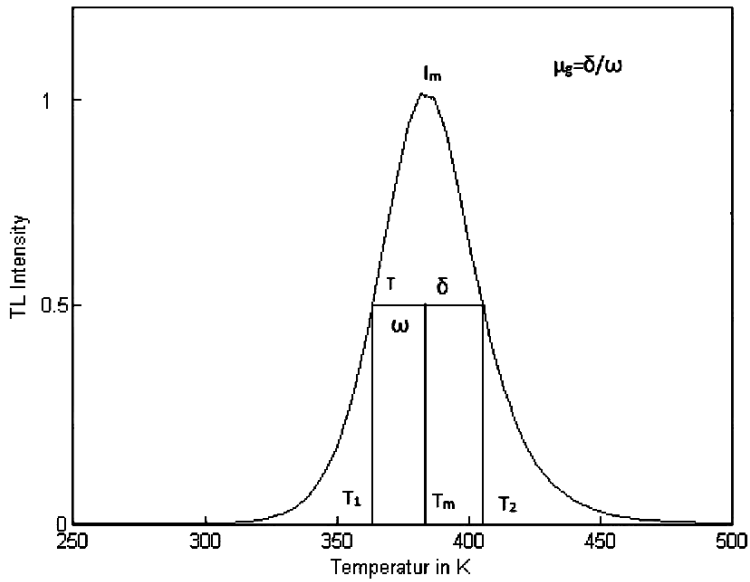

Fig. 1
A synthetic glow peak.

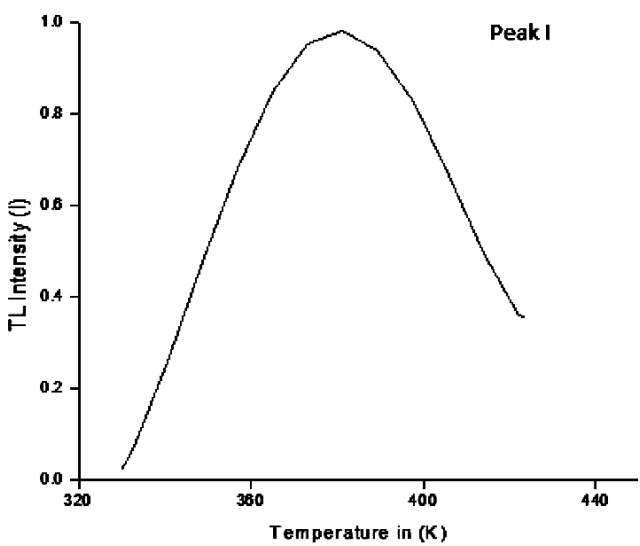

Fig. 2
Normalized isolated *TL* peak of Sodalite(Peak-I).

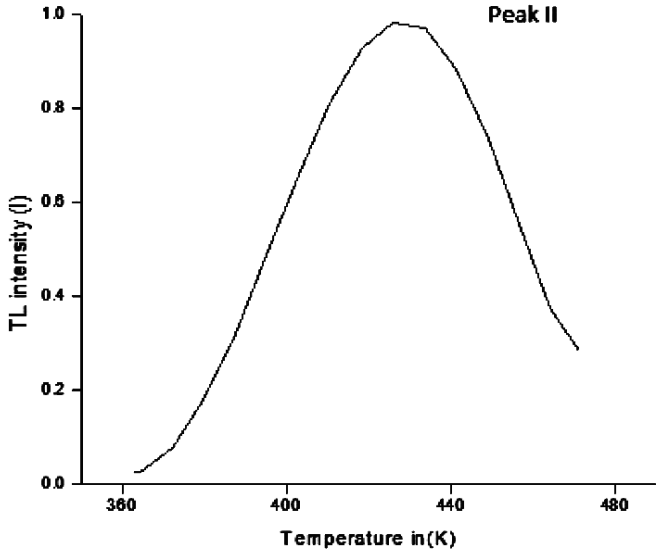

Fig. 3
Normalized isolated *TL* peak of Sodalite(Peak-II).

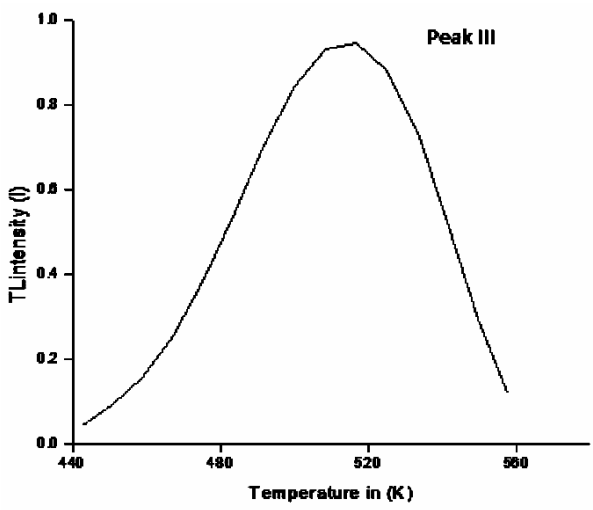

Fig. 4
Normalized isolated *TL* peak of Sodalite(Peak-III).

4. Conclusion

In the conventional peak shape method usually the half intensity points are used. But normally clean *TL* peaks do not occur. As a result there is some overlap from neighbouring peaks. But if we use the points such as $x = 2/3$ and $4/5$ corresponding to upper half of the *TL* peak the effect of overlapping can be reduced there by increasing the accuracy of the values of activation energies. In view of this we have extended the conventional peak shape method by deriving the formulas of activation energy corresponding to the points $x = 2/3$ and $4/5$ in the upper half of the peak. Finally the applicability of the expression of activation energy has been checked by applying them both to computer generated *TL* peaks and experimental *TL* peaks of Sodalite and encouraging results have been obtained.

Acknowledgement

One of our authors (SA) thanks Dr. T.S.C. Singh and Prof. R. K. Gartia for their help and thanks are due to the refree for his comments.

References

1. Chen, R. and Mckeever, S.W.S.− Theory of Thermoluminescence and Related Phenomena, World Scientific, Singapore (1997).
2. Chen, R. and Pagonis, V.− Thermally and Optically Stimulated Luminescence: A Simulation Approach, Wiley UK (2011).
3. Fleming, R. J.− Can. J. Physics, **46**,1509 (1968).
4. Singh, W. S., Singh, S.J. Deb, N.C., Bhattachrya, M., Singh, S.D. and Majumdar, P.S.– Indian, J. Phys., **72A**, 163 (1998).
5. Singh, T.S.C. – Ph.D. Thesis , Manipur University, Imphal, India (1989).
6. Singh, S.D. – Ph.D. Thesis, Manipur University, Imphal, India (1994).
7. Garlik, G.F.G. and Gibson, A.F.− Proc. Phys. Soc., **40**, 574 (1948).
8. Das, B.C. and Mukherjee, B.N.− Differential Calculas, U.N. Dhar and Sons, Kolkata, India (2012).
9. Randall, J.J. and Wilkins, M.H. F.− Proc. Roy. Soc., **A184**, 390 (1945).
10. Abramwitz, M. and Stegun, J. A.− Hand Book of Mathematical Functions, Dover : New York (1965).
11. Singh, S.J., Karmakar, M., Bhattacharya, M., Singh, S.D., Singh, W.S. and Azharuddin, SK. – Indian J. Physics, **86**, 113 (2012).
12. Spigel, M. R. and Slephens, L. J. − Third edition, Tata McGraw Hill Publishing Company, New Delhi, India (2000).

INDIAN JOURNAL OF THEORETICAL PHYSICS, VOL. 65, NOS. 1 & 2, 2017

Effect of Hall current on radiating and chemically reacting MHD oscillatory slip flow in a planner channel with varying temperature and concentration with suction/injection

Satya Sagar Saxena
Associate Professor in Mathematics,
IILM College of Engineering and Technology, Greater Noida-201306, U.P., India
E-mail: satya.saxena@iilmcet.ac.in; drsaagar2310@gmail.com

(Received for publication in February, 2017)

[**Abstract :** An investigation of the combined influence of Hall effects and chemical reaction on the flow of unsteady *MHD* mixed convective oscillatory flow of an electrically conducting optically thin fluid through a planer channel filled with saturated porous medium is carried out. The effect of Hall current, heat source, thermal radiation and chemical reaction of the fluid were taken into considerations with slip boundary condition, varying temperature and concentration. The closed-form analytical solutions are obtained for the momentum, energy and concentration equations. The velocity, temperature, and concentration profiles are evaluated numerically and presented graphically using MATLAB for different values of flow parameters.]

Key words : Hall Current; Chemical reaction; Oscillatory flow; Heat Source; Radiation

1. Introduction

The significance of *MHD* convection flows through porous media is far reaching in heat and mass transfer problems and has received rigorous attention in recent studies involving diverse fields like thermal generator, nuclear reactors, geothermal energy extractions and in the field of aerodynamics. Oscillatory flows simultaneously find their use in diverse engineering fields. In addition, Hall effects on the fluid flow with variable concentration play a major role in the field of power generators and accelerators in geophysics, in design of underground water energy storage system, soil sciences, astrophysics, nuclear power reactors and so on.

Oscillatory flows has known to result in higher rates of heat and mass transfer, many studies have been done to understand its characteristics in different systems such as reciprocating engines, pulse combustors and chemical reactors. Cramer and Pai[1] taken transverse applied magnetic field and magnetic Reynolds number are assumed to be very small, so that the induced magnetic field is negligible. Muthucumaraswamy, et. al.[2] have studied the effect of homogenous chemical reaction of first order and free convection on the oscillating infinite vertical plate with variable temperature and mass diffusion. Sharma[3] investigate the effect of periodic heat and mass transfer on the unsteady free convection flow past a vertical flat plate in slip flow regime when suction velocity oscillates in time. Chaudhary and Jha[4] studied the effects of chemical reactions on *MHD* micro polar fluid flow past a vertical plate in slip flow regime. Anjali Devi, et. al.[5] have examined the effect of chemical reaction on the flow in the presence of heat transfer and magnetic field. Muthucumaraswamy, et. al.[6] have investigated the effect of thermal radiation effects on flow past an impulsively started infinite isothermal vertical plate in the presence of first order chemical reaction.

Moreover, Al-Odat and Al-Azab[7] studied the influence of magnetic field on unsteady free convective heat and mass transfer flow along an impulsively started semi infinite vertical plate taking into account a homogeneous chemical reaction of first order. The effect of radiation on the heat and fluid flow over an unsteady stretching surface has been analyzed by El-Aziz[8]. Singh, et. al.[9] studied the heat transfer over stretching surface in porous media with transverse magnetic field. Singh, et. al.[10,11] also investigated *MHD* oblique stagnation-point flow towards a stretching sheet with heat transfer for steady and unsteady cases. Elbashbeshy, et. al.[12] investigated the effects of thermal radiation and magnetic field on unsteady boundary layer mixed convection flow and heat transfer problem from a vertical porous stretching surface.

The chemical reaction, heat and mass transfer on *MHD* flow over a vertical stretching surface with heat source and thermal stratification have been presented by Kandasamy, et. al.[13]. The opposing buoyancy effects on

simultaneous heat and mass transfer by natural convection in a fluid saturated porous medium investigated by Angirasa, et. al.[14]. Ahmed[15] investigates the effects of unsteady free convective *MHD* flow through a porous medium bounded by an infinite vertical porous plate. Ahmed Sahin[16] studied the magneto hydrodynamic and chemical reaction effects on unsteady flow, heat and mass transfer characteristics in a viscous, incompressible and electrically conduction fluid over a semi infinite vertical porous plate in a slip-flow regime. V. Sri Hari Babu and G. V. Ramana Reddy[17] analyzed the mass transfer effects on *MHD* mixed convective flow from a vertical surface with Ohmic heating and viscous dissipation. Satya Sagar Saxena and Dubey[18] studied the effects of *MHD* free convection heat and mass transfer flow of visco-elastic fluid embedded in a porous medium of variable permeability with radiation effect and heat source in slip flow regime. Unsteady *MHD* heat and mass transfer free convection flow of polar fluids past a vertical moving porous plate in a porous medium with heat generation and thermal diffusion was analyzed by Satya Sagar Saxena and Dubey[19].

Sudeerbabu, et. al.[20] analyzed the radiation and chemical reaction effects on an unsteady *MHD* convective flow past a vertical moving porous plate embedded in a porous medium with viscous dissipation. Unsteady *MHD* free convection flow and mass transfer near a moving vertical plate in the presence of thermal radiation is studied by Seethamahalakshmi, et. al.[21].

Ahmed, et. al.[22] studied the unsteady *MHD* free convection flow past a vertical porous plate with thermal diffusion, heat source and Hall current. They showed that the decrease in the Soret effect leads to an increase in both main flow and cross flow velocity. Hall effect is found to decrease the main flow velocity near the plate and increase the cross flow velocity.

Effects of radiation and Hall current on *MHD* flow of a viscous, Newtonian and electrically conducting fluid past a porous rotating infinite disk was investigated by Anjali Devi[23]. They showed that the increase in magnetic interaction lead to decrease in radial, tangential and axial velocities but results in increased temperature distribution while a decrease

in the hall parameter reduces the tangential velocity and temperature distribution. An investigation on hall effect with a chemically reacting flow for an oscillatory *MHD* convective, viscous, incompressible, radiating and electrically conducting fluid in a vertical porous rotating channel in slip flow regime was studied by Chand, et. al.[24]. Recently, Joseph, et. al.[25] have studied the chemical reaction effects on unsteady *MHD* oscillatory slip flow in an optically thin fluid through a planer channel in the presence of a temperature-dependent heat source.

In this paper, we have studied the effect of Hall current on radiating and chemically reacting *MHD* oscillatory slip flow in a planner channel with varying temperature and concentration in the presence of suction/injection. The closed form solutions for velocity, temperature, skin friction, concentration, Nusselt number, and Sherwood number are presented. The effects of pertinent parameters on fluid flow of heat and mass transfer characteristics are studied in detail and presented graphically using MATLAB and discussed qualitatively.

2. Flow description and governing equations

We consider the unsteady mixed convection, two dimensional slip flow of an electrically conducting, heat generating, optically thin and chemically reacting oscillatory fluid flow in a planer channel filled with porous medium in the presence of thermal radiation with temperature and concentration variation. Take a Cartesian coordinate system (x', y') where x'-axis is taken along the flow and y'-axis is taken normal to the flow direction. A uniform transverse magnetic field of magnitude B_0 which is strong enough to produce Hall current is applied in the presence of thermal and Solutal buoyancy effects in the direction of y'-axis. Then, taking into account Boussinesq's approximation, heat source, radiation and Hall effects in the incompressible viscous flow, the governing equations for the momentum, energy and concentration are given as follows :

$$\frac{\partial v'}{\partial y'} = 0 \qquad \ldots \quad (1)$$

$$\frac{\partial u'}{\partial t'} = -\frac{1}{\rho}\frac{\partial p'}{\partial x'} + \nu\frac{\partial^2 u'}{\partial y'^2} + g\beta(T' - T_1') + g\beta^*(C' - C_1') - \left[\frac{\nu}{K'} + \frac{\sigma B_0^2}{\rho(1+m^2)}\right]u' - v'\frac{\partial u'}{\partial y'} \qquad \ldots \quad (2)$$

$$\frac{\partial T'}{\partial t'} = \frac{k}{\rho C_p}\frac{\partial^2 T'}{\partial y'^2} - \frac{1}{\rho}\frac{\partial q_r'}{\partial y'} + Q\frac{(T'-T_1')}{\rho C_p} - v'\frac{\partial T'}{\partial y'} \quad \ldots \quad (3)$$

$$\frac{\partial C'}{\partial t'} = D\frac{\partial^2 C'}{\partial y'^2} - K_r'(C' - C_1') - v'\frac{\partial C'}{\partial y'} \quad \ldots \quad (4)$$

where $v' = -v_0(1 + \varepsilon e^{i\omega t})$ is suction velocity.

The appropriate boundary conditions are

$$u' = L_1\frac{\partial u'}{\partial y'},\ T' = T_1' + \delta_T^*\frac{\partial T'}{\partial y'},\ C' = C_1' + \delta_C^*\frac{\partial C'}{\partial y'} \text{ at } y' = 0 \quad \ldots \quad (5)$$

$$u' = 0,\ T' = T_2' + \delta_T^*\frac{\partial T'}{\partial y'},\ C' = C_2' + \delta_C^*\frac{\partial C'}{\partial y'} \quad \text{at } y' = d \quad \ldots \quad (6)$$

where u', v' – the velocity components in the x', y' − directions respectively, p' − the pressure, ν − the kinematic viscosity, k − the thermal conductivity, β − the coefficient of volume expansion due to temperature, β^* − the coefficient of volume expansion due to concentration, ρ − the density, σ −the electrical conductivity of the fluid, g−the acceleration due to gravity, T−the temperature, T'_1 − the wall temperature of the fluid, q'_r − the radiative heat flux, C' −the concentration, C'_1 −the wall concentration of the fluid, K'_r − chemical reaction coefficient, L_1 − mean free path, C_p − specific heat at a constant pressure, m− the Hall current parameter, K' − the permeability of the porous medium, Q−the coefficient of heat source and D−the mass diffusivity.

Cogley, et. al.[26] have shown that, for the optically thin fluid flow, radiative heat flux is represented by the following form :

$$\frac{\partial q_r'}{\partial y'} = 4(T_1' - T)I' \text{ , where } I' = \int_0^\infty K_{\lambda w}\frac{\partial e_{b\lambda}}{\partial T}d\lambda \quad \ldots \quad (7)$$

where $K_{\lambda w}$ is the radiation absorption coefficient at the wall and $e_{b\lambda}$ is Plank constant.

Introducing the following non-dimensional quantities :

$$x = \frac{x'}{d},\ y = \frac{y'}{d},\ p = \frac{dp'}{\mu u_0},\ u = \frac{u'}{u_0},\ \theta = \frac{T'-T_1'}{T_2-T_1},$$

$$\phi = \frac{C'-C_1'}{C_2-C_1},\ t = \frac{u_0 t'}{d},\ Re = \frac{u_0 d}{\nu},\ \gamma = \frac{K'}{d^2}$$

$$M = \frac{\sigma B_0^2 d^2}{\mu},\ Gr = \frac{g\beta(T_2 - T_1)d^2}{\nu u_0},\ Gr = \frac{g\beta^*(C_2 - C_1)d^2}{\nu u_0},$$

$$R = \frac{4l'd^2}{k},\ Pe = \frac{\rho C_p u_0 d}{k},\ Sc = \frac{D}{u_0 d},$$

$$Kr = \frac{K_r' d}{u_0},\ d_2 = \frac{\delta_T^*}{d},\ d_1 = \frac{\delta_C^*}{d},\ K' = Kd^2 \quad \ldots \quad (8)$$

In view of the above dimensionless variables, the basic field equations (2) to (4) can be expressed in non-dimensionless form as

$$Re\frac{\partial u}{\partial t} = -\frac{\partial p}{\partial x} + \frac{\partial^2 u}{\partial y^2} + \lambda_1\frac{\partial u}{\partial y} + Gr\theta + Gc\phi - \left(\frac{M}{1+m^2} + \frac{1}{K}\right)u \quad \ldots \quad (9)$$

$$Pe\frac{\partial \theta}{\partial t} = \frac{\partial^2 \theta}{\partial y^2} + Pe\lambda_2\frac{\partial \theta}{\partial y} + \left(C_p R + \alpha\right)\theta \quad \ldots \quad (10)$$

$$\frac{\partial \phi}{\partial t} = Sc\frac{\partial^2 \phi}{\partial y^2} + \lambda_3\frac{\partial \phi}{\partial y} - Kr\,\phi \quad \ldots \quad (11)$$

The corresponding boundary conditions for m > 0 are transformed to

$$\left.\begin{aligned} u &= \gamma\frac{\partial u}{\partial y},\ \theta = d_2\frac{\partial \theta}{\partial y},\ \phi = d_1\frac{\partial \phi}{\partial y} && \text{at } y = 0 \\ u &= 0,\ \theta = 1 + d_2\frac{\partial \theta}{\partial y},\ \phi = 1 + d_1\frac{\partial \phi}{\partial y} && \text{at } y = 1 \end{aligned}\right\} \quad \ldots \quad (12)$$

where *p*, *Re*, *M*, *K*, *Pe*, *R*, *Sc*, λ, d_1, d_2, *Gr*, *Gc* and γ are pressure, Reynolds number, magnetic parameter, permeability parameter, Peclet number, thermal radiation parameter, Schmidt number, real constant, volumetric concentration expansion, volumetric thermal expansion, thermal Grashof number, solutal Grashof number and slip parameter respectively.

3. Solution of the problem

In order to solve equations (9) $-$(11) with respect to the boundary conditions (12) for purely oscillatory flow, let us take

$$u(y,t) = u_0(y)e^{i\omega t} \quad \ldots \quad (13)$$

$$\theta(y,t) = \theta_0(y)e^{i\omega t} \quad \ldots \quad (14)$$

$$\phi(y,t) = \phi_0(y)e^{i\omega t} \quad \ldots \quad (15)$$

$$-\frac{\partial p}{\partial x} = e^{i\omega t} \quad \ldots \quad (16)$$

Substituting the equations (13) − (16) in equations (9) − (12), we obtain

$$u_0''(y) + a_1 u_0'(y) - a_2 u_0 = -(\lambda + Gr\theta_0 + Gc\phi_0) \quad \ldots (17)$$

$$\theta_0''(y) + a_5 \theta_0'(y) + a_6 \theta_0 = 0 \quad \ldots (18)$$

$$\phi_0''(y) + a_3 \phi_0'(y) - a_4 \phi_0 = 0 \quad \ldots (19)$$

where prime denotes ordinary differentiation with respect to *y*.

The corresponding boundary conditions can be written as

$$\left.\begin{array}{ll} u_0 = \gamma u_0',\ \theta_0 = d_2\theta_0',\ \phi_0 = d_1\phi_0' & \text{at } y = 0 \\ u_0 = 0,\ \theta_0 = 1 + d_2\theta_0',\ \phi_0 = d_1\phi_0' & \text{at } y = 1 \end{array}\right\} \quad \ldots (20)$$

Solving equations (17) − (19) under the boundary conditions (20), we obtain the velocity, temperature and concentration distribution in the boundary layer as

$$u_0(y,t) = A_1 e^{m_1 y} + A_2 e^{m_2 y} + K_1 + K_2 e^{m_5 y} + K_3 e^{m_6 y} + K_4 e^{m_3 y} + K_5 e^{m_4 y}$$

$$\theta_0(y,t) = A_5 e^{m_5 y} + A_6 e^{m_6 y}$$

$$\phi_0(y,t) = A_3 e^{m_3 y} + A_4 e^{m_4 y}$$

where

$$K_1 = \frac{\lambda_1}{a_2},\ K_2 = \frac{-GrA_5}{m_5^2 + a_1 m_5 - a_2},\ K_3 = \frac{-GrA_6}{m_6^2 + a_1 m_6 - a_2},\ K_4 = \frac{-GcA_3}{m_3^2 + a_1 m_3 - a_2},\ K_5 = \frac{-GcA_4}{m_4^2 + a_1 m_4 - a_2},$$

$$A_1 = \frac{K_{14}}{K_{12}} - \frac{K_{13}}{K_{12}} K_{18},\ A_2 = K_{18},\ A_3 = \frac{-K_{20}\sin n\pi}{K_{19}},\ A_4 = \sin n\pi,\ A_5 = \frac{-K_7}{K_7 K_8 - K_6 K_9},$$

$$A_6 = \frac{-K_6}{K_7 K_8 - K_6 K_9}, m_1 = \frac{-a_1 + \sqrt{a_1^2 - 4a_2}}{2}, m_2 = \frac{-a_1 - \sqrt{a_1^2 - 4a_2}}{2},$$

$$m_3 = \frac{-a_3 + \sqrt{a_3^2 + 4a_4}}{2}, m_4 = \frac{-a_3 - \sqrt{a_3^2 + 4a_4}}{2}, m_5 = \frac{-a_5 + \sqrt{a_5^2 - 4a_6}}{2}, m_6 = \frac{-a_5 - \sqrt{a_5^2 - 4a_6}}{2},$$

$$a_1 = \lambda_1, a_2 = \frac{M}{1+m^2} + \frac{1}{K} + i\omega Re, a_3 = \frac{\lambda_3}{Sc}, a_4 = \frac{Kr + i\omega}{Sc}, a_5 = Pe\lambda_2, a_6 = C_p R + \alpha - Pei\omega$$

$$K_6 = 1 - d_2 m_5,\ K_7 = 1 - d_2 m_6,\ K_8 = (e^{m_5} - m_5 e^{m_5}),\ K_8 = (e^{m_6} - m_6 e^{m_6}),$$

$K_{10} = K_1 + K_2 + K_3 + K_4 + K_5,\ K_{11} = \gamma(K_2 m_5 + K_3 m_6 + K_4 m_3 + K_5 m_4),$

$K_{12} = (1 - \gamma m_1),\ K_{13} = (1 - \gamma m_2),\ K_{14} = K_{11} - K_{10},$

$K_{15} = K_1 + K_2 e^{m_5} + K_3 e^{m_6} + K_4 e^{m_3} + K_5 e^{m_4},\ K_{16} = e^{m_1},\ K_{17} = e^{m_2}$

$K_{18} = \frac{K_{14} K_{16} + K_{12} K_{15}}{K_{13} K_{16} - K_{12} K_{17}}, K_{19} = 1 - d_1 m_3, K_{20} = 1 - d_1 m_4.$

The shear stress, the coefficient of the rate of heat transfer and rate of mass transfer at any point in the fluid can be characterized by

$\tau^* = -\mu \frac{\partial u}{\partial y},\ Nu^* = -k \frac{\partial T}{\partial y},\ Sh^* = -D \frac{\partial C}{\partial y}$

In dimensional form

$\tau = \frac{\tau^* d}{\mu u_0} = -\frac{\partial u}{\partial y},\ Nu = -\frac{Nu^* d}{x(T_1 - T_0)} = -\frac{\partial \theta}{\partial y},\ Sh = -\frac{Sh^* d}{C_1 - C_0} = -\frac{\partial \phi}{\partial y}.$

The skin-friction (τ), the Nusselt number (Nu) and the Sherwood number (Sh) at the walls $y = 0$ and $y = 1$ are given by

$\tau_0 = \left(-\frac{\partial u}{\partial y}\right)_{y=0}, \qquad \tau_1 = \left(-\frac{\partial u}{\partial y}\right)_{y=1},$

$Nu_0 = \left(-\frac{\partial \theta}{\partial y}\right)_{y=0}, \qquad Nu_1 = \left(-\frac{\partial \theta}{\partial y}\right)_{y=1},$

$Sh_0 = \left(-\frac{\partial \phi}{\partial y}\right)_{y=0}, \qquad Sh_1 = \left(-\frac{\partial \phi}{\partial y}\right)_{y=1}.$

4. Results and discussions

In order to get a physical insight into the problem the effects of various governing parameters on the velocity profile, temperature profile, and the concentration profile are computed and represented in Figures 1-10 and discussed in detail for the different values of the flow parameters involved in the governing equations *e.g.* the Hall parameter *m*, the magnetic parameter *M*, the Grash of number *Gc*, the permeability of the porous medium parameter *K*, the frequency of oscillation ω, the thermal radiation

parameter R, the heat source parameter α, the Schmidt number Sc, the volumetric concentration expansion d_1, and the chemical radiation parameter Kr. The graphs were plotted using MATLAB where only the real parts of the equations were considered. Throughout the computations the values used were, $t = 1$, $M = 2$, $Re = 1$, $Gr = 5$, $Gc = 2$, $R = 2$, $\alpha = 3$, $Pe = 4$, $Kr = 2$, $g = 0.1$, $d_1 = 0.002$, $d_2 = 0.002$, $\omega = 0.5$, $Sc = 0.22$ except where a parameter is varied.

In Fig. 1, the variation of u with different values of Hall parameter m is displayed. It is seen that, an increase in the Hall parameter enhances u in the region. Fig. 2 illustrates the effect of magnetic field on the velocity profiles. When the applied magnetic field intensity increases, there seems to be a decrease in the velocity field. It is true as the magnetic force retards the flow, velocity decreases. The effect of modified Grashof number Gc on the velocity field has been represented in Fig. 3. It is observed that as the modified Grashof number increases the velocity field increases. Fig. 4 depicts the velocity profiles for various values of permeability parameter K. It is seen that an increase in the permeability parameter results in an increase in the fluid velocity. In Fig. 5, it is noticed that an increase in the frequency of oscillation ω shows a decrease in the velocity profile. Temperature profiles are displayed through figures 6 −7. Fig. 6 depicts the temperature profiles with the variations in radiation parameter R. It is clear that the fluid temperature $\theta(y, t)$ decreases with an increase in radiation parameter R. This result qualitatively agrees with expectations, since the effect of radiation decrease the rate of energy transport to the fluid, thereby decreasing the temperature of the fluid. The effect of heat source parameter α on the temperature field is illustrated in Fig.7. It is observed that as α increases, the temperature decreases. Concentration profiles are represented in figures 8 − 10. In Fig 8, increase in the Schmidt number Sc increases the species concentration (mass transfer). In Fig 9, increase in the concentration variation parameter decreases the fluid concentration. In Fig 10, increase in the chemical radiation parameter decreases the concentration profile.

Effect of Hall parameter *m* on velocity

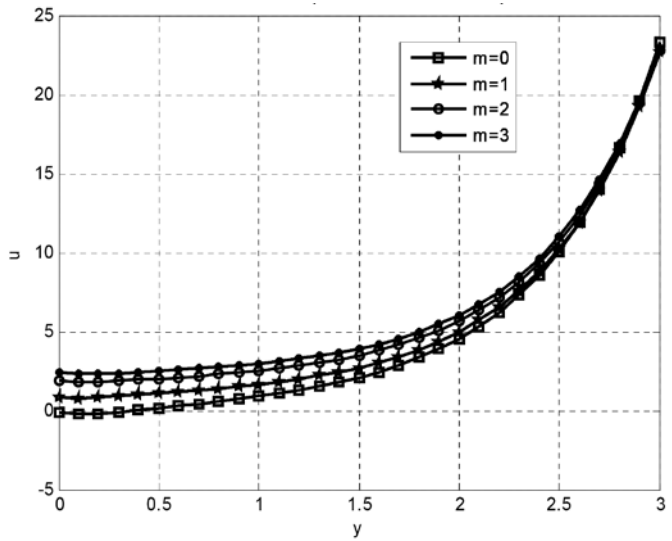

Fig. 1
Variation of *u* with *m*.

Effect of Hartmann number *m* on velocity

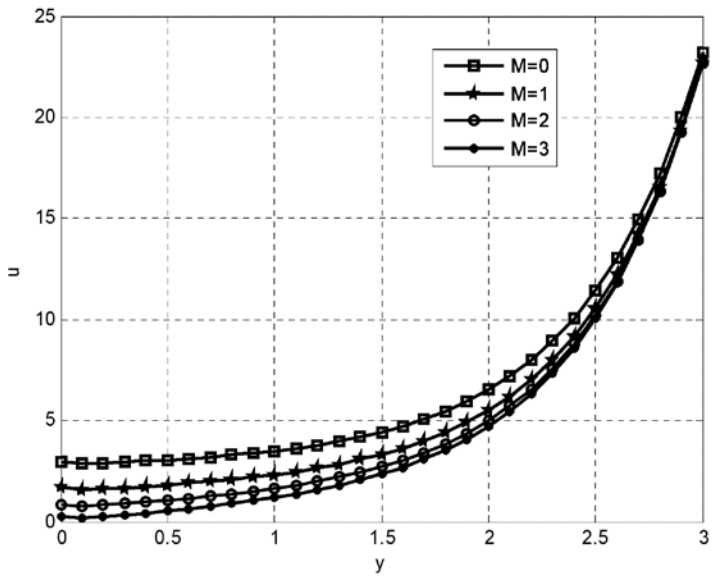

Fig. 2
Variation of *u* with *M*.

Effect of solutal Grashof number *Gc* on velocity

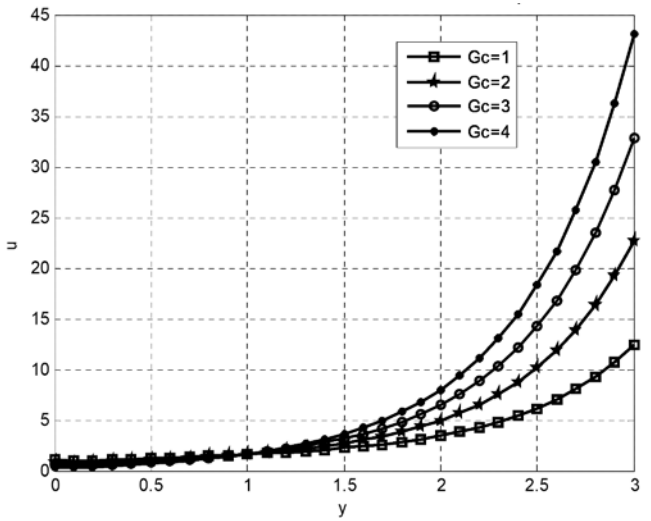

Fig. 3

Variation of *u* with *Gc.*

Effect of permeability parameter *K* on velocity

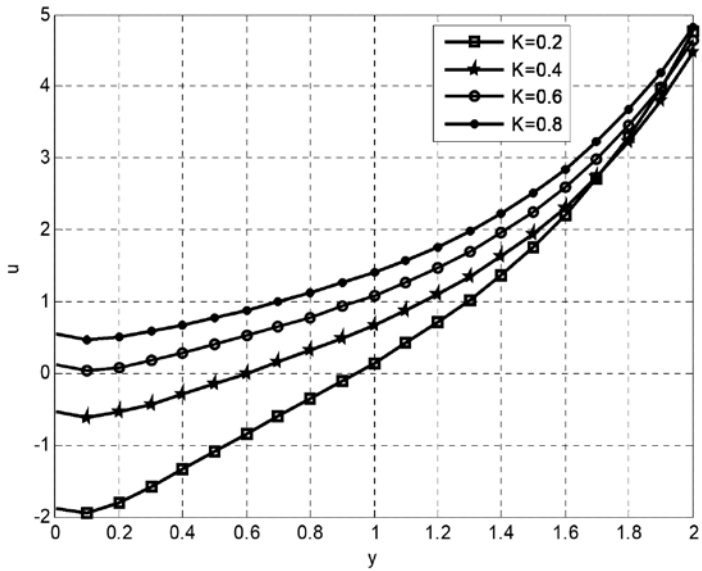

Fig. 4

Variation of *u* with *K.*

Effect of frequency oscillation ω on velocity

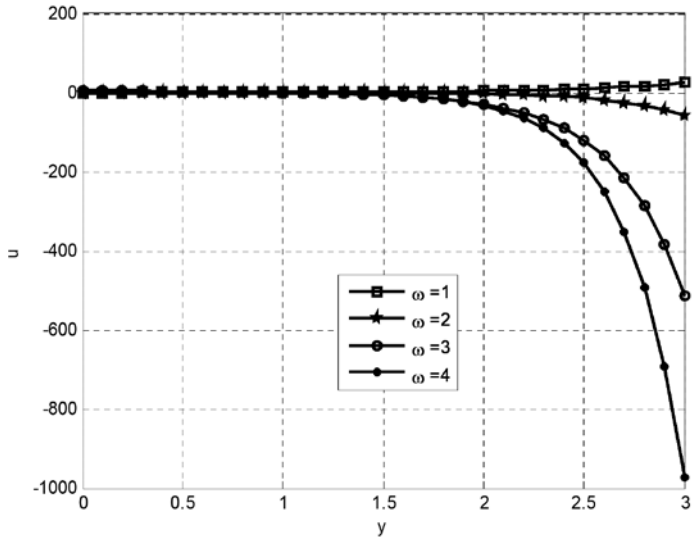

Fig. 5

Variation of u with ω.

Effect of thermal radiation parameter R on temperature

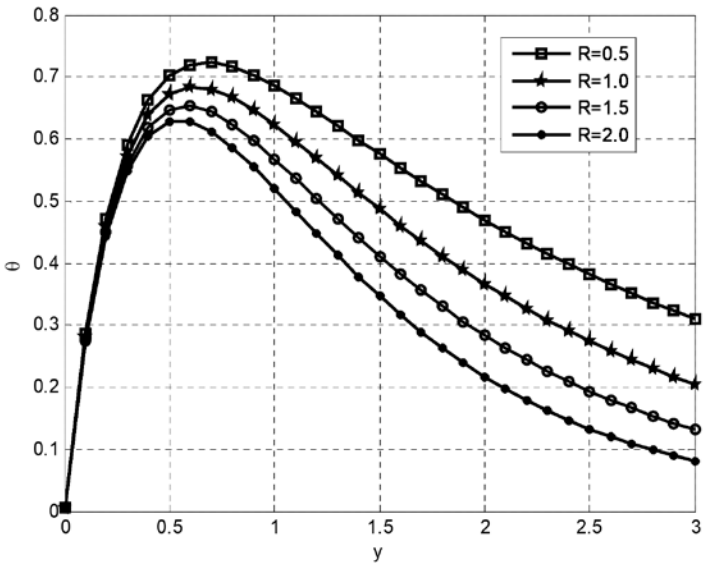

Fig. 6

Variation of θ with R.

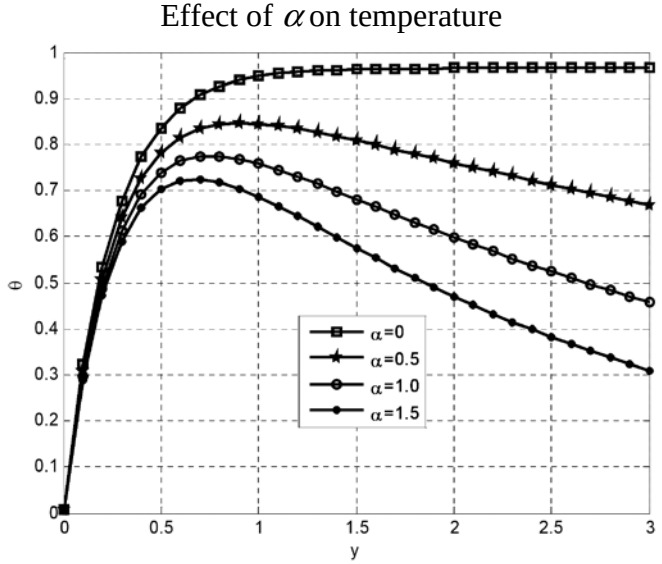

Fig. 7
Variation of θ with α.

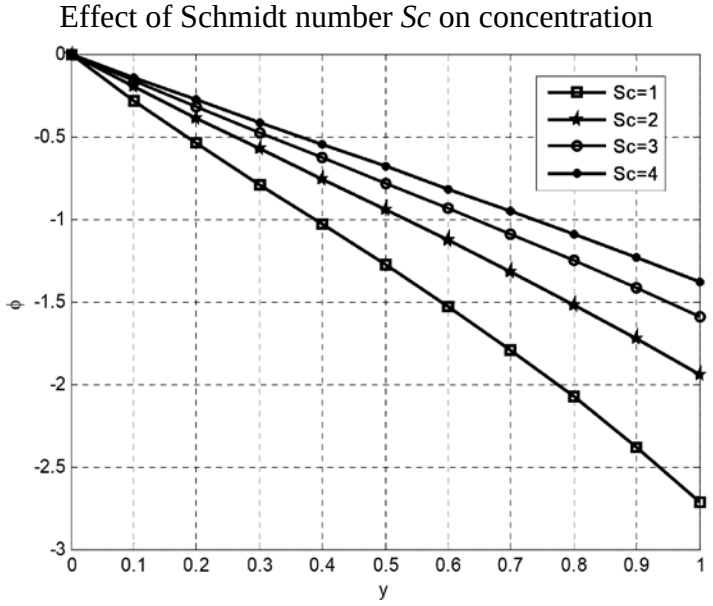

Fig. 8
Variation of ϕ with Sc.

Effect of d_1 on concentration

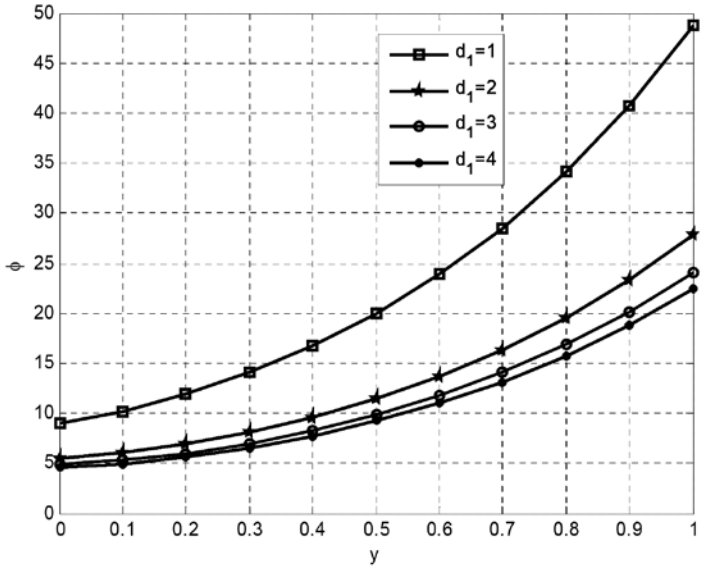

Fig. 9
Variation of ϕ with d_1.

Effect of Kr on concentration

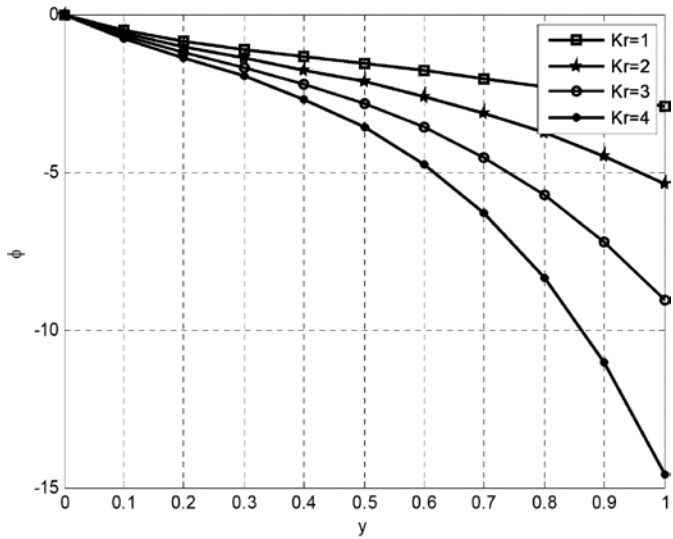

Fig. 10
Variation of ϕ with Kr.

References

1. Cramer, K. R. and Pai, S. I. − Magneto fluid dynamics for Engineering and Applied Physicists (McGraw Hill, New York), (1973).
2. Muthucumaraswamy, R. and Meenakshisundaram, S.− Theoret. Appl. Mech., Vol. **33**, No. 3, pp. 245-257, (2006).
3. Sharma, P. K.− Latin American Applied Research, **35**, 313-319, (2005).
4. Chaudhary, R. C. and Jha, A. K. − Applied Mathematics and Mechanics, **29** (9), 1179-1194, (2008).
5. Anjali Devi, S.P. and Kandasamy, R.− Z. Angew. Math. Mech., **80**, 697-701,(2000).
6. Muthucumaraswamy, R. and Chandrakala, P.− Jour. of Applied Mechanics and Engineering, Vol. **11,** No. 3, pp 639-646, (2006).
7. Al-Odat, M. Q. and Al-Azab,− Emirates J. Engg. Res.,**12** (3), 15-21, (2007).
8. El-Aziz, M.A.− International Communications in Heat and Mass Transfer, Vol. **36**, pp 521-524, (2009).
9. Singh, P., Tomer, N.S. and Sinha, D.− Proceeding of International Conference on Challenges and application of Mathematics in Sciences and Technology, ISBN 023-032-875-X, pp 422-430, (2010).
10. Singh, P., Tomer, N.S., Kumar, S. and Sinha, D.− International Journal of Applied Mathematics and Mechanics, Vol. **6**, No.13, pp 94-111, (2010).
11. Singh, P., Jangid, A.,Tomer, N.S., Kumar, S. and Sinha, D.− International Journal of Information and Mathematical Sciences, Vol.**6**, No.3, pp 63-69, (2010).
12. Elbashbeshy, E. M. A., Yassmin, D. M. and Dalia, A. A.− African Journal of Mathematics and Computer Science Research, Vol. **3**, No.5, pp 68-73, (2010).
13. Kandasamy, R., Periasamy, K. and Sivagnana Prabhu, K.K.− Int. J. Heat and Mass Transfer, **48** (21-22), 4557-4561, (2005).
14. Angirasa, D., Peterson, G. P. and Pop, I.− Int. J. Heat Mass Trans., **40**(12), 2755-2773, (1997).
15. Ahmed, S.− Bull. Cal. Math. Soc., **99** (5), 511-522, (2007).
16. Ahmed Sahin,− Emirates Journal for Engineering Research, **15** (1), 25-34, (2010).
17. Sri Hari Babu, V. and Ramana Reddy, G. V.− Advances in Applied Science Research, **2** (4), 138-146, (2011).
18. Saxena, Satya Sagar and Dubey, G. K.− Advances in Applied Science Research, **2** (5), 115-129, (2011).
19. Saxena, Satya Sagar and Dubey, G. K.− Advances in Applied Science Research, **2** (4), 259-278, (2011).

20. Sudheer Babu, M., Satya Narayana, P. V., Sankar Reddy, T. and Umamaheswara Reddy, D.− Advances in Applied Science Research, **2** (5), 226-239, (2011).

21. Seethamahalakshmi, Ramana Reddy G.V. and Prasad, B.D.C.N. − Advances in Applied Science Research, Vol. **2**(6), pp. 261-269, (2011).

22. Ahmed, N., Kalita, H. and Barua, D. P.− Int. J. of Engg., Sci. and Tech., Vol. **2**, No. 6, pp. 59-74, (2010).

23. Anjali Devi, S. P. and Uma Devi, R.− Journal of Applied Fluid Mechanics, Vol. **5**, No. 2, pp. 1-7, (2012).

24. Chand. K., Singh, K. D. and Kumar, S.− Adv. in Appl. Sci. Res., Vol. **3**, No. 4, pp. 2424-2437, (2012).

25. Joseph, K.M., Ayuba, P., Yusuf, L.H., Mohammed, S.M. and Ayok, I. − J., International Journal of Scientific Engineering and Applied Science, Vol.**1**, Issue-5, (2015).

26. Cogely, A.C., Vicent, W.G. and Giles, S.E.− Differential approximation to radiative heat transfer in a non-grey near equilibrium.. AIAA J, pp.551-553, (1968).

INDIAN JOURNAL OF THEORETICAL PHYSICS, VOL. 65, NOS. 1 & 2, 2017

Possibility of metal–insulator transition in a special type of Hubbard superlattice

Jayeeta Chowdhury
Department of Physics, Scottish Church College,
1, Urquhart Square, Kolkata - 700006, India
E-mail: jyt_ch@yahoo.com, jcphys@scottishchurch.ac.in

(Received for publication in March, 1017)

[**Abstract**: A brief study of the ground state of a one dimensional Hubbard superlattice with $-B-B-A-$ type of unit cell is presented in this paper. Self consistent Hartree Fock Approximation calculation and real space renormalization group technique are used for this study. Possible metal–insulator transition points are found out after investigation of the energy gap for various combinations of on–site Coulomb repulsion energies.

Key words: Superlattice, Renormalization group, Hartree Fock Approximation, Metal Insulator transition

1. Introduction

Multilayered structures or superlattices show exciting features like oscillation of exchange coupling, giant magnetoresistance etc[1–3]. These materials are very useful in nanoelectronic devices. Intense theoretical attempt was made to understand the behaviour of such systems using simple one dimensional superlattices as model[4–14]. The present work contains a study of the ground state of a half-filled one dimensional $-B-B-A-$ Hubbard superlattice. Hartree Fock Approximation method and Renormalization Group technique are used for the study. Detailed investigation of the energy gap of the system gives indication of the possibility of metal–insulator transition under certain conditions. Ground state phase diagram indicating the phase transition has been drawn.

The model

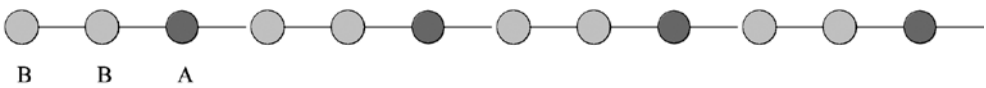

Fig. 1
One dimensional – *B* – *B* – *A* – Hubbard superlattice.

The model is a one dimensional superlattice with unit cell size three. Unit cell pattern is – *B* – *B* – *A* –. For this present work, site potential energies for all sites are zero and only nearest neighbour hopping (*t*) is considered. The model Hamiltonian is

$$H = t\sum_{i,\sigma}(c^{+}_{i,\sigma}c_{i+1,\sigma} + h.c.) + U_i\sum_{i} n_{i\uparrow}n_{i\downarrow} \quad \ldots \quad (1)$$

$c^{+}_{i,\sigma}\left(c_{i,\sigma}\right)$ is the creation (annihilation) operator for an electron with spin $\sigma\left(\uparrow,\downarrow\right)$ at the *i*th site. $n_{i,\sigma} = c^{+}_{i,\sigma}c_{i,\sigma}$ and $n_i = \sum_{\sigma} n_{i,\sigma}$,the number operator at the *i*th site. For half–filled band $\sum_{i} n_i = N$ (the number of sites). U_i is the on–site Coulomb repulsion energy at the *i*th site, which follows a repeated pattern depending on the unit cell. Scale of energy is chosen by setting $t = 1.0$.

2. The Methods

Hartree Fock Approximation (HFA) Method : In the *HFA*, the Coulomb terms are substituted in the following way ($\alpha = A, B$)

$$U_\alpha n_{i\uparrow}n_{i\downarrow} \rightarrow U_\alpha\langle n_{i\uparrow}\rangle n_{i\downarrow} + U_\alpha n_{i\uparrow}\langle n_{i\downarrow}\rangle - U_\alpha\langle n_{i\uparrow}\rangle\langle n_{i\downarrow}\rangle \quad \ldots \quad (2)$$

Now the up and the down spin terms in the Hamiltonian are decoupled. In an unrestricted *HFA*, Hamiltonians can be diagonalised in a self-consistent manner to obtain the single particle energy levels. The ground state is constructed by filling up the energy levels of both the up and the down bands up to the Fermi level.

Energy gap at the Fermi level is given by

$$\Delta_{HFA} = E_{n+1} + E_{n-1} - 2E_n \quad \ldots \quad (3)$$

where E_n is the ground state energy of the *n* electron system.

Renormalization Group (RG) Technique: In this scheme, the whole chain is divided into non-overlapping cells containing three sites (*–B–B–A–*). Now the Hamiltonian contains an intracell (H_0) part and an intercell (T) part. The intracell part (H_0) contains the site energies, the Hubbard terms and also the hopping terms describing electron transfer within the cell; it is a sum of all cell Hamiltonians. The intercell part (T) contains the hopping energy corresponding to the transfer of electrons from one cell to the adjacent ones.

For one site, there are four possible states *viz.* $|0\rangle$, $c_{\uparrow}^{+}|0\rangle \equiv |+\rangle$, $c_{\downarrow}^{+}|0\rangle \equiv |-\rangle$, $c_{\uparrow}^{+}c_{\downarrow}^{+}|0\rangle \equiv |\pm\rangle$. Therefore for one cell, there are 64 possible states. For the study of half–filled case only the subspaces

$$\{n = 2,\ S = S_z = 0\},$$

$$\left\{n = 3,\ S = \frac{1}{2},\ S_z = \pm\frac{1}{2}\right\}$$

and

$$\{n = 4,\ S = S_z = 0\}$$

are needed. Cell Hamiltonians are diagonalised for these subspaces and only the lowest energy states are retained. These four states in a cell are now identified as the 'renormalized' on–site states : $|0'\rangle$, $|+'\rangle$, $|-'\rangle$, $|\pm'\rangle$

In the truncated basis, the intracell Hamiltonian is

$$H_0' = E_2 + (E_3 - E_2)(n_{\uparrow}' + n_{\downarrow}') + (E_4 + E_2 - 2E_3)n_{\uparrow}'n_{\downarrow}' \ . \qquad \ldots \quad (4)$$

Here E_4, E_3 and E_2 are the lowest energies of the subspaces corresponding to four, three and two electrons respectively. From this relation renormalized on–site quantities (Coulomb potential and site potential) follow as

$$U' = E_4 + E_2 - 2E_3, \quad \varepsilon' = E_3 - E_2 \qquad \ldots \quad (5)$$

And the gap in the energy spectrum Δ_{RG} is the magnitude of U at the last stage of iteration.

To find the renormalized hopping matrix elements, the matrix elements of c_{σ}^{b} between the renormalized on–site states are calculated, where c_{σ}^{b} is the annihilation operator of the electron with spin σ at the boundary site of the cell.

$$\langle 0' | c_{\uparrow}^{b} | +' \rangle = \lambda_1, \qquad \langle -' | c_{\uparrow}^{b} | \pm' \rangle = \lambda_2 .$$

Since this model possesses spin reversal symmetry, elements for $c^b_{\downarrow}$ will be as same as that of $c^b_{\uparrow}$ (except for a fermionic sign change in the value of λ). The approximation $\lambda = \sqrt{|\lambda_1 \lambda_2|}$ leads to $c^b_{\sigma} = \lambda c'_{\sigma}$, which in turn leads to effective renormalized hopping $t' = \lambda^2 t$.

3. *The Result*

Using both the methods mentioned above the energy gap of the system has been studied. For *HFA* calculation convergence with the system size was checked. Here the *HFA* result with N = 120 under periodic boundary condition is presented. For both *HFA* and *RG* calculations U_A/t and U_B/t are varied from 0.0 to 5.0. Energy gap (Δ) values clearly indicate the metallic ($\Delta \sim 0.0$ or $\Delta \sim 1/N$) or insulating (Δ large) behaviour of the system.

After detailed investigation of the energy gap the $U_A/t - U_B/t$ phase diagram is plotted.

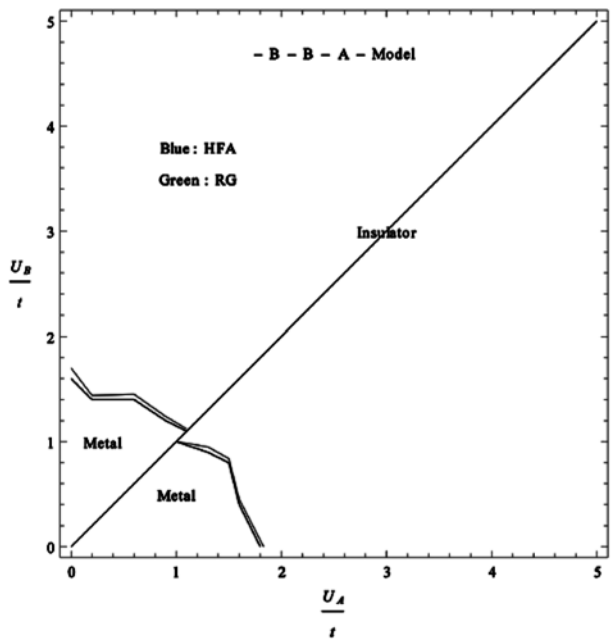

Fig. 2

Phase diagram showing metallic and insulating phases. Red line corresponds to perfect spin ordered phase. Blue and green phase boundaries correspond to *HFA* and *RG* calculations respectively. *HFA* results are for N = 120.

When $U_A/t = U_B/t$, the system is perfectly spin ordered (*SO*). For low but unequal U_A/t and U_B/t values (range ~ 0.0 to 1.5) the system shows metallic behaviour.

For other combinations of U_A/t and U_B/t the system is insulating (*SO*).This behaviour indicates a metal–insulator transition in the system. The different phases and the transition lines are clearly indicated on the diagram. Superposition of the results obtained from *HFA* and *RG* shows good agreement. Though both the methods are approximate, their agreement indicates that the results are quite reliable.

4. Conclusion

Summarizing, the paper contains the study of a one dimensional half-filled $-B-B-A-$ Hubbard superlattice at ground state using *HFA* and *RG* techniques. The results obtained by two methods match quite well. Possible combinations of U_A/t and U_B/t values are found out which will lead to metal–insulator transition within this system. It is a unique property for this special system. This behaviour may be used to devise a correlation controlled switch and may have many applications in technology. Further investigation (both theoretical and experimental) of this system under various external conditions, such as electric field, magnetic field etc. will be very much interesting.

References

1. Heinrich, B. and Cochran, J. F. – Adv. Phys., **42**, 523 (1993).
2. Parkin, S. S. P., More, N. and Roche, K. P. – Phys. Rev. Lett., **64**, 2304 (1990).
3. Baibich, M. N., Broto, J. M., Fert, A., Nguyen, Van Dau F., Petroff, F., Etienne, P., Creuzet, G., Friederich, A. and Chazelas, J. – Phys. Rev. Lett., **61**, 2472 (1988).
4. Paiva, T. and dos Santos, R. R. – Phys. Rev. Lett., **76**, 1126 (1996).
5. Paiva, T. and dos Santos, R. R. – Phys. Rev., B**58**, 9607 (1998).
6. Paiva, T. and dos Santos, R. R. – Phys. Rev., B **65**, 153101 (2002).
7. Malvezzi, A. L., Paiva, T. and dos Santos, R. R. – Phys. Rev., B **73**, 193407 (2006).
8. Silva-Valencia, J., Miranda, E. and dos Santos, R. R. – J. Phys.: Condens. Matter, **13**, L609 (2001).
9. Kakashvili, P. and Japaridze, G. I. – J. Phys.: Condens. Matter, **16**, 5815 (2004).

10. Gupta, S., Sil, S. and Bhattacharyya, B. – Phys. Rev., B **63**, 125113 (2001).
11. Chowdhuy, J., Karmakar, S. N. and Bhattacharyya, B. – Phys. Rev., B **75**, 235117 (2007).
12. Chowdhuy, J., Karmakar, S. N. and Bhattacharyya, B. – J. Phys.: Condens. Matter, **21**, 15302 (2009).
13. Chowdhury, J. – Indian Journal of Theoretical Physics, **64,** 53 (2016).
14. Chowdhury, J. – International Journal of Pure and Applied Physics, **13**, 271 (2017).

INDIAN JOURNAL OF THEORETICAL PHYSICS, VOL. 65, NOS. 1 & 2, 2017

A mathematical model of non-Newtonian fluid : an innovative study

Arun Kumar Maiti

Assistant Professor in Mathematics,
Shyampur Siddheswari Mahavidyalaya,
Ajodhya, Howrah
E-mail : dr.arun.maiti@gmail.com

(Received for publication in March, 2017)

[**Abstract:** The aim of the present analysis is to study the non-Newtonian behaviour of blood in presence of arterial stenosis. Assuming that the stenosis is mild the expressions for flux, dimensionless resistance to flow and wall shear stress have been studied here. The numerical results are shown graphically and discussed.]

Key words: Herschel-Bulkley fluid, wall shear stress, flow rate, resistance to flow and stenosis.

1. Introduction

It is well known that the nature of blood flow is deflected from its original state due to the presence of arterial stenosis. So the size of the stenosis plays a vital role in blood flow through stenosed artery. Though from the pathological stand point of view, actual formation of stenosis remains unclear to us , it is assumed that stenosis is formed by the deposition or accumulation of fatty substances in the inner wall of the artery and the abnormal growth of the connective tissue. This may be caused due to unhealthy living conditions, such as exposure to tabacco smoke, lack of physical activity and improper dietary habits. Many cardiovascular diseases, such as hypertension, atherosclerosis, heart attack and brain hemorrhage are influenced by the presence of arterial stenosis. So the hydrodynamical factors such as wall shear stress, resistance to flow etc. can play a significant role in the progression and development of this pathological conditions.

In view of this, many authors have presented various types of mathematical models for blood flow to study the flow characteristics

through stenosed artery (Young[1], Lee and Fung[2], Shukla, et. al[3], Chaturani and Samy[4]). In all the above studies, blood has been considered as a Newtonian fluid. But since blood is a suspension of cells in plasma, Majhi and Nair[5] suggested that under certain conditions blood behaves like a non-Newtonian fluid. Many researchers have used the Casson fluid model for mathematical modelling of blood flow to study the non-Newtonian behaviour of blood (Blair[6], Charm and Kurland[7]). Chaturani and Samy[8] have presented a purterbation fluid model to analyze the pulsatile flow of Casson fluid through stenosed artery. Jain, et. al.[9] have studied a mathematical model of blood through an irregular arterial stenosis and they have observed that if the viscosity of fluid increases the velocity of fluid decreases in presence of stenosis. Biswas, et. al.[10] have studied two-layered pulsatile flow of blood through an arterial tube by considering the core layer as Bingham plastic fluid and the peripheral layer as Newtonian fluid. Aroesty and Gross[11] have developed a Casson fluid theory for pulsatile flow through narrow uniform artery. Parmar, et. al.[12] have analysed a mathematical model to show the effect of stenosis on Casson flow of blood. Tu and Deville[13] have investigated the pulsatile flow of blood in stenosed arteries. Some authors have presented mathematical models (Maruthiprasad and Radhakrishnamacharya[14], Siddiqui, et al.[15], Biswas, et. al.[16]) by considering blood as a Herschel-Bulkley type non-Newtonian fluid.

In the presented study I propose to discuss the effects of stenosis on Herschel- Bulkley flow of blood.

2. Mathematical formulation

Let us consider the steady flow of blood through an axially symmetric but radially non symmetric stenosed artery.

The geometry of stenosis[17] can be defined as

$$\frac{R}{R_0} = 1 - \frac{\delta}{2R_0}\left[1 + \cos\frac{2\pi}{l_0}\left(z - d - \frac{l_0}{2}\right)\right], \; d \le z \le d + l_0$$

$$= 1, \qquad \text{otherwise} \qquad \ldots \quad (1)$$

where R_0 is the radius of the artery in the normal region, δ is the height of the stenosis and R is the radius in the stenotic region, l_0 is the length of the stenosis and d indicates the location of the stenosis.

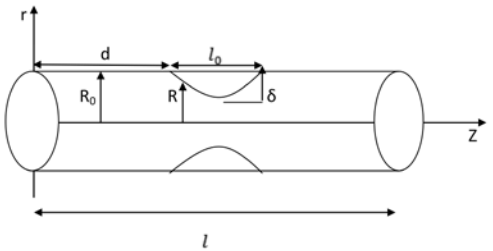

Fig. 1
Schematic diagram of artery with stenosis.

The equation of motion is given by

$$-\frac{dp}{dz} = \frac{1}{r}\frac{d}{dr}(r\tau) \qquad \ldots \quad (2)$$

In case of Herschel-Bulkley flow, the relationship between shear stress and shear rate is given by

$$\tau = \mu\left(-\frac{\partial w}{\partial r}\right)^n + \tau_0,\ \tau \geq \tau_0\ \ -\frac{\partial w}{\partial r} = 0,\ \tau < \tau_0 \qquad \ldots \quad (3)$$

From which we get

$$-\frac{\partial w}{\partial r} = \left(\frac{\tau - \tau_0}{\mu}\right)^{1/n}$$

Boundary conditions are

$w = 0$ at $r = R(z)$

τ is finite at $r = 0$

Integrating (2) we get

$$\tau = -\frac{r}{2}\frac{dp}{dz} + \frac{4}{r}$$

Since τ is finite at $r = 0$, we get $A = 0$

Thus $$\tau = -\frac{r}{2}\frac{dp}{dz}$$

The wall shear stress τ_w is given by

$$\tau_w = -\frac{R}{2}\frac{dp}{dz}, \text{ where } R = R(z)$$

The volumetric flow rate *i.e.* the flux is given by

$$Q = \int_0^R 2\pi r w \, dr \qquad \ldots \quad (4)$$

Integrating (4) and using no slip condition we get

$$Q = 2\pi \int_0^R (-\frac{\partial w}{\partial r}).\frac{r^2}{2} \, dr$$

$$= \pi \int_0^R (\frac{\tau - \tau_0}{\mu})^k r^2 \, dr \text{ , where } k = 1/n$$

Now $$\frac{\tau}{\tau_w} = \frac{r}{R}$$

⇨ $$dr = \frac{R}{\tau_w} \, d\tau$$

Thus $$Q = \frac{\pi R^3}{\mu^k \tau_w^3} \int_0^{\tau_w} (\tau - \tau_0)^k \tau^2 \, d\tau$$

$$= \frac{\pi R^3 \tau_w^k}{\mu^k} \left[\frac{\left(1 - \frac{\tau_0}{\tau_w}\right)^{k+1}}{k+1} - \frac{2\left(1 - \frac{\tau_0}{\tau_w}\right)^{k+2}}{(k+1)(k+2)} \right.$$

$$\left. + \frac{2}{(k+1)(k+2)(k+3)} \left\{ \left(1 - \frac{\tau_0}{\tau_w}\right)^{k+3} - \left(-\frac{\tau_0}{\tau_w}\right)^{k+3} \right\} \right]$$

When $\frac{\tau_0}{\tau_w} \ll 1$, we get

$$Q = \frac{\pi R^3 \tau_w^k}{\mu^k (k+3)} \left[1 - \frac{k(k+3)}{(k+2)} \frac{\tau_0}{\tau_w}\right]$$

$$= \frac{\pi R^3}{\mu^k (k+3)} \left[\tau_w - \frac{k+3}{k+2} \tau_0\right]^k$$

$$\Rightarrow \quad \tau_w = \{\frac{Q\,(k+3)}{\pi R^3}\}^{\frac{1}{k}} \mu + \frac{k+3}{k+2} \tau_0 \qquad \ldots \quad (5)$$

So $$-\frac{dp}{dz} = -\frac{2(k+3)}{k+2} \frac{\tau_0}{R} - \{\frac{Q\,(k+3)}{\pi}\}^{\frac{1}{k}} \frac{2\mu}{R^{(\frac{3}{k}+1)}}$$

Now $p = p_1$ at z = 0 and $p = p_2$ at z = l, so we get

$$p_1 - p_2 = \frac{2(k+3)}{(k+2)} \frac{\tau_0}{R_0} \int_0^l (\frac{R}{R_0})^{-1} dz + \{\frac{Q\,(k+3)}{\pi}\}^{\frac{1}{k}} \frac{2\mu}{R_0^{\left(\frac{3}{k}+1\right)}} \int_0^l (\frac{R}{R_0})^{-\left(\frac{3}{k}+1\right)} dz, \ldots (6)$$

where $\frac{R}{R_0}$ can be obtained from (1).

The resistance to flow λ is defined by

$$\lambda = \frac{2(k+3)}{(k+2)}\frac{\tau_0}{R_0 Q}\left[l - l_0 + 2\int_0^{\pi}\frac{d\theta}{a-bcos\theta}\right] + \left\{\frac{Q\,(k+3)}{\pi Q^k}\right\}^{\frac{1}{k}}\frac{2\mu}{R_0^{\left(\frac{3}{k}+1\right)}}\left[2\int_0^{\pi}\frac{d\theta}{(a-bcos\theta)^{\left(\frac{3}{k}+1\right)}} + l - l_0\right]$$

In the absence of stenosis the resistance to flow λ_N is given by

$$\lambda_N = \frac{2(k+3)}{(k+2)}\frac{\tau_0}{R_0 Q}\,l + \left\{\frac{Q\,(k+3)}{\pi Q^k}\right\}^{\frac{1}{k}}\frac{2\mu l}{R_0^{\left(\frac{3}{k}+1\right)}}$$

In dimensionless form the resistance to flow λ is given by

$$\overline{\lambda} = \frac{\lambda}{\lambda_N} = 1 - \frac{l_0}{l} + \frac{1}{l}\frac{\frac{2(k+3)}{(k+2)}\frac{\tau_0}{R_0 Q}I_1 + \left\{\frac{Q\,(k+3)}{\pi Q^k}\right\}^{\frac{1}{k}}\frac{2\mu}{R_0^{\left(\frac{3}{k}+1\right)}}I_2}{\frac{2(k+3)}{(k+2)}\frac{\tau_0}{R_0 Q} + \left\{\frac{Q\,(k+3)}{\pi Q^k}\right\}^{\frac{1}{k}}\frac{2\mu}{R_0^{\left(\frac{3}{k}+1\right)}}} \quad \ldots \quad (7)$$

where $$I_1 = 2\int_0^{\pi}\frac{d\theta}{a-bcos\theta}$$

$$I_2 = 2\int_0^{\pi}\frac{d\theta}{(a-bcos\theta)^{\left(\frac{3}{k}+1\right)}},$$

$$a = 1 - \frac{\delta}{2R_0}, b = \frac{\delta}{2R_0}$$

Again in the absence of stenosis the wall shear stress can be written as

$$\tau_N = \left\{\frac{Q\,(k+3)}{\pi R_0^3}\right\}^{\frac{1}{k}}\mu + \frac{k+3}{k+2}\tau_0$$

In dimensionless form, the wall shear stress may be written as

$$\overline{\tau_w} = \frac{\tau_w}{\tau_N} = \frac{\left\{\frac{Q\,(k+3)}{\pi R_0^3}\right\}^{\frac{1}{k}}\mu\left(\frac{R}{R_0}\right)^{-3/k} + \frac{k+3}{k+2}\tau_0}{\left\{\frac{Q\,(k+3)}{\pi R_0^3}\right\}^{\frac{1}{k}}\mu + \frac{k+3}{k+2}\tau_0} \quad \ldots \quad (8)$$

3. *Numerical discussions*

To illustrate the flow analysis the results are shown graphically with the help of MATLAB-7.6. Figures 2 and 3 give the variation of flux for different values of θ and yield stress with the variations of $\frac{\delta}{R_0}$. It is observed that Q increases with the increase of $\frac{\delta}{R_0}$, but the reverse effect occurs when θ and yield stress τ_0 increases.

Figures 4 and 5 illustrate the behaviour of resistance to flow for different values of yield stress τ_0 and stenosis length l_0. It is found that resistance to flow increases with the increase of $\frac{\delta}{R_0}$, but the reverse effect occurs when yield stress τ_0 and stenosis length l_0 increase.

Figures 6 and 7 depict the variation of wall shear stress for different values of θ and yield stress τ_0. It is clear from the figure that the wall shear stress $\overline{\tau_w}$ increases with the increase of $\frac{\delta}{R_0}$ and yield stress, but it decreases with the increase of θ.

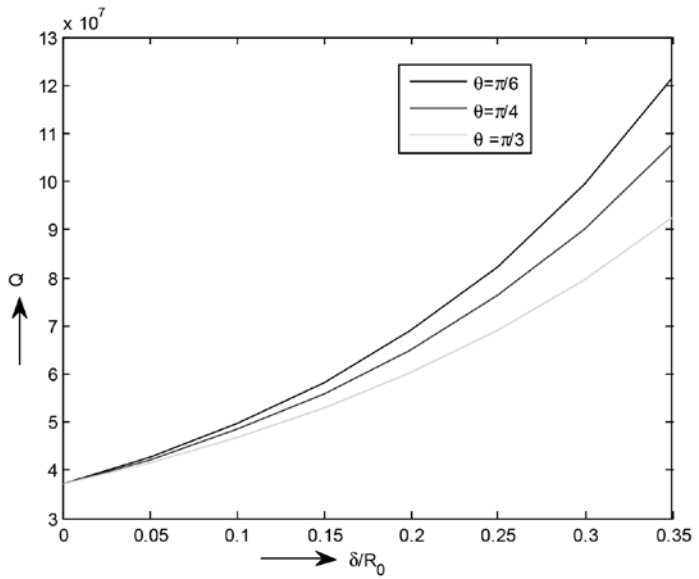

Fig. 2

Variation of flux Q for different values of θ with the variation of $\frac{\delta}{R_0}$.

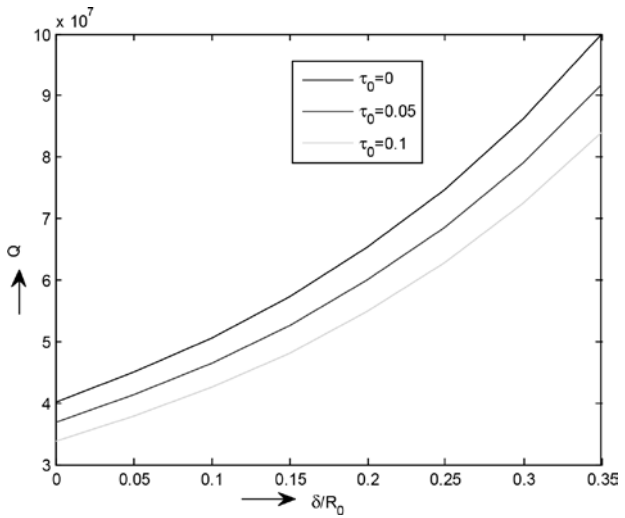

Fig. 3

Variation of flux Q for different values of yield stress τ_0 with the variation of $\frac{\delta}{R_0}$.

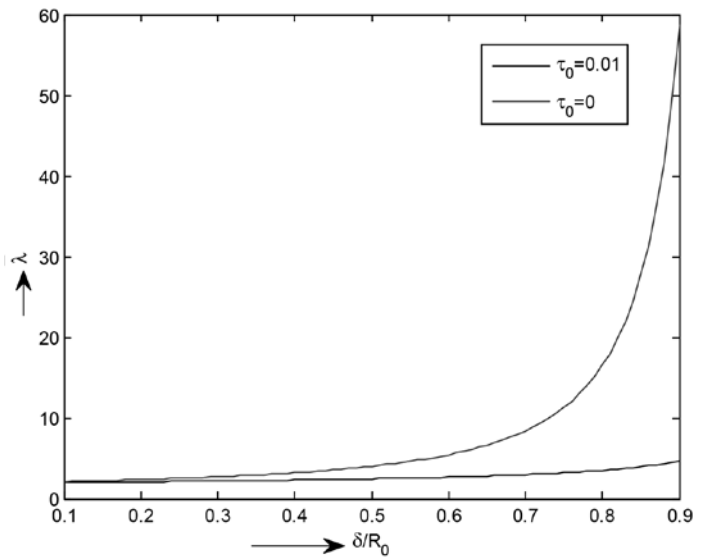

Fig. 4

Fluctuation of non -dimensional resistance to flow λ for different values of yield stress τ_0 with the variation of $\frac{\delta}{R_0}$.

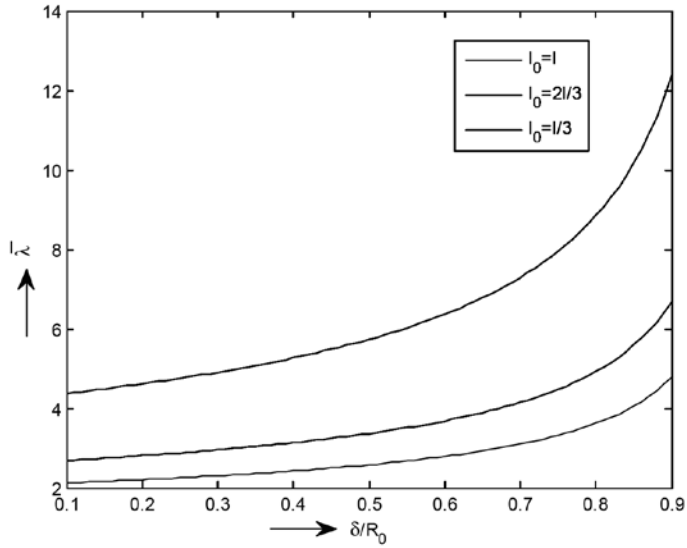

Fig. 5

Fluctuation of non-dimensional resistance to flow λ for different values of Stenosis length l_0 with the variation of $\frac{\delta}{R_0}$.

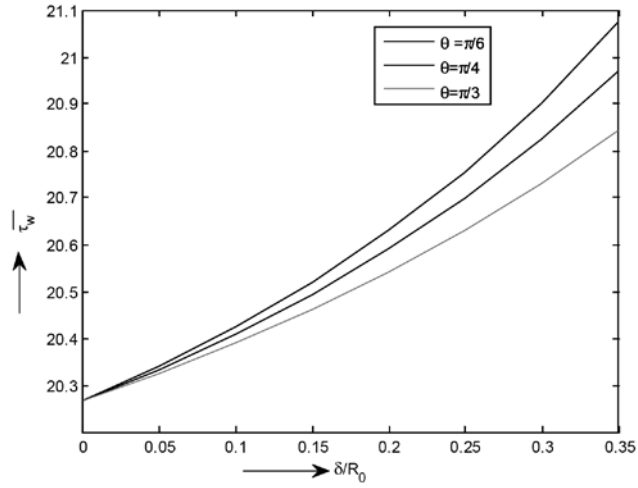

Fig. 6

Variation of non-dimensional wall shear stress $\overline{\tau_w}$ for different values of θ with the variation of $\frac{\delta}{R_0}$.

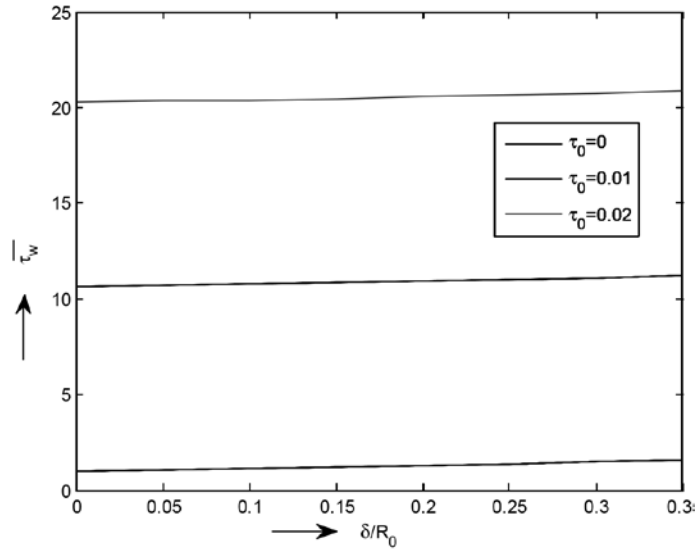

Fig. 7

Variation of non-dimensional wall shear stress $\overline{\tau_w}$ for different values of yield stress τ_0 with the variation of $\frac{\delta}{R_0}$.

4. Conclusions

Blood flow through an artery mainly depends on the flux , wall shear stress and resistance to flow. Here the solutions have been shown for mild stenosis. It is observed that flux is varying markedly across the stenotic region. If the stenotic size increases, wall shear stress and resistance to flow increase. Thus the results are greatly influenced by the change of stenosis and shape parameter. So the present analysis may be helpful for better understanding and prevention of arterial diseases**.**

References

1. Young, D. F. −Effects of a time-dependent stenosis on flow through a tube, J. Engrg. Ind. Trans. ASME, Vol. **90**, 248-254, (1968).
2. Lee, J. S. and Fung, Y. C.− Flow in locally constricted tubes and low Reynolds numbers **,** J. Appl. Mech., Trans, ASME, Vol. **37**, 9-16, (1970).

3. Shukla, J. B., Parihar, R.S. and Rao, B,R.P.− Effects of stenosis on non-Newtonian flow through an artery with mild stenosis, Bull. Math. Biol., Vol. **42**, 283-294, (1980).

4. Chaturani, P. and PonnalagarSamy, V. R.− Pulsatile flow of Casson's fluid through stenosed arteries with applications to blood flow, Biorheol., Vol. **23**, 499-511, (1986).

5. Majhi, S.N. and Nair, V. R.− Pulsatile flow of third grade fluids under body acceleration- modelling blood flow, Int. J. Engg. Sci., Vol. **32**(5), 839-846, (1996).

6. Blair, G. W. S.− An equation for the flow of blood, plasma serum through glass capillaries, Nature, Vol. **183** (4661), 613-614, (1959).

7. Charm, S. and Kurland, G.− Viscometry of human blood for shear rates of 0-100000 sec^{-1}, Nature, Vol**. 206** (4984), 614-618, (1965).

8. Chaturani, P. and PonnalagarSamy, V. R.− A Study of non-Newtonian aspects of blood flow through stenosed arteries and its applications in arterial disease, Biorheology, Vol**. 22** (6), 521-531, (1985).

9. Jain, M., Sharma, G. C. and Sharma, S. K.− A mathematical model for blood flow through narrow vessels with mild stenosis, IJE Transactions B. Applications, Vol. **22**(1), 99-106, (2009).

10. Biswas, D. and Chakraborty, U. S.− Two layered pulsatile blood flow in a stenosed artery with body acceleration and slip at wall, applications and Applied mathematics, An International Journal (AAM), Vol. **5** (2), 303-320, (2010).

11. Aroesty, J. and Gross, J. F.− Pulsatile flow in small blood vessels, I. Casson Theory, Biorheology, Vol**. 9**(1), 33-43, (1972).

12. Parmar, L., Kulshrestha, S. B. and Singh, D. P.− Effects of stenosis on Casson flow of blood through arteries, Int. J. of Advanced Computer and Mathematical Sciences, Vol. **4**(4), 257- 268, (2013).

13. Tu, C. and Deville, M.− Pulsatile flow of non-Newtonian fluid through arterial stenosis, J. Biomech., Vol**. 29**, 899-908, (1986).

14. Maruthiprasad, K. and Radhakrishnamacharya, G.− Flow of Herschel-Bulkley fluid through an inclined tube of non-uniform cross section with multiple stenosis, Arch. Mech.,Warszawa, Vol. **60** (2), 161-172, (2008).

15. Siddqui, S. U., Verma, W. K. and Gupta, R. S.− A Mathematical model for pulsatile flow of Herschel-Bulkley fluid through stenosed arteries, Journal of Sc. and Technology, Vol**. 4**(5), 49-66, (2010).

16. Biswas, D. and Laskar, R. B.− Steady flow of blood through a stenosed artery : A non-Newtonian fluid model, Assam University Journal of Sci. and Tech. Vol. **7**(11), 144-153, (2011).

17. Kumar, S. and Diwakar, C.− A Mathematical model of power law fluid with an application of blood flow through an artery with stenosis, Advances in Applied Mathematical Biosciences Vol. **4**(2), 51-61, (2013).

INDIAN JOURNAL OF THEORETICAL PHYSICS, VOL. 65, NOS. 1 & 2, 2017

Libration points of a cable-connected satellites system in elliptical orbit under several influences of general nature

Sangam Kumar
P. G. Department of Physics, L. S. College,
B. R. A. Bihar University, Muzaffarpur- 842001, India
Mobile No.: +91-9905222295
E-mail: kumarsangam.phy@gmail.com

(Received for publication in April, 2017)

[**Abstract:** The aim of the present work is to study the libration points of the motion of a system of two artificial satellites connected by a light, flexible, inextensible and non-conducting cable under the influence of solar radiation pressure, shadow of the earth, earth's magnetic field and air resistance. We discuss the case of elliptical orbit of centre of mass of the system. We derive differential equations of motion of the system. Jacobian integral of the system has also been obtained. Thereafter libration points of the motion of the system have been obtained.]

Key words: Satellites system, Libration points, Elliptical orbit.

1. Introduction

The libration points of the motion of a system of two cable-connected artificial satellites under the influence of solar radiation pressure, earth's magnetic field, shadow of the earth and air resistance is studied. The influence of the above mentioned perturbations on the system has been studied singly and by a combination of any two or three of them by various workers, but never conjointly all at a time. Therefore, these could not give a real picture of motion of the system. This fact has initiated the present research work. The case of elliptical orbit of the centre of mass of the system is discussed. Shadow of the earth is taken to be cylindrical and the system is allowed to pass through the shadow beam. The satellites are connected by a light, flexible, inextensible and non-conducting cable. The satellites are taken as charged material particles. Since masses of the satellites are small and distances between the satellites and other celestial

bodies are very large, the gravitational forces of attraction between the satellites and other celestial bodies including the sun have been neglected.

The present work is an attempt towards the generalization of work done by Beletsky and Novikova[1] and Beletsky and Novoorebelskii[2]. They studied the motion of a system of two satellites connected by a light, flexible and inextensible string in the central gravitational field of the earth relative to its centre of mass. This study assumed that the two satellites are moving in the plane of the centre of mass. Das, et. al.[3] studied the effect of magnetic force on the motion of a system of two cable-connected satellites in orbit. Kumar and Bhattacharya[4] studied the stability of equilibrium positions of two cable-connected satellites under the influence of solar radiation pressure, earth's oblateness and earth's magnetic field. Kumar, et. al.[5,6] obtained the equations of motion of a system of two cable-connected artificial satellites under the influence of solar radiation pressure, earth's oblateness and shadow of the earth. Singh and Demin[7] and Singh[8] investigated the problem in two and three dimensional cases.

2. Treatment of the problem

Equations of motion of one of the satellites when the centre of mass moves along Keplerian elliptical orbit in Nechvill's co-ordinate system[9] are written as Kumar[6]

$$X''-2Y'-3X\rho=\lambda_a X-\frac{A}{\rho}\cos i-\gamma\left(\frac{B_1}{m_1}-\frac{B_2}{m_2}\right).\cos\in\cos(\nu-\alpha)-f\rho\rho'$$

and

$$Y''+2X'=\lambda_a Y-\frac{A\rho'}{\rho^2}\cos i+\gamma\left(\frac{B_1}{m_1}-\frac{B_2}{m_2}\right).\cos\in\sin(\nu-\alpha)-f\rho^2 \quad \ldots (1)$$

with the condition of constraint

$$X^2+Y^2\le\frac{1}{\rho^2} \quad \ldots (2)$$

Also

$$\rho=\frac{1}{(1+e\cos\nu)},$$

$$\lambda_a=\frac{p^3\rho^4}{\mu}\left(\frac{m_1+m_2}{m_1m_2}\right)\lambda=\rho^4\beta,$$

$$\beta = \frac{p^3}{\mu}\left(\frac{m_1+m_2}{m_1 m_2}\right)\lambda,\ A = \left(\frac{m_1}{m_1+m_2}\right)\left(\frac{Q_1}{m_1}-\frac{Q_2}{m_2}\right)\frac{\mu_E}{\sqrt{\mu\rho}}$$

$$f = \frac{a_1 p^3}{\sqrt{\mu p}},\ a_1 = \rho_a R'(c_2 - c_1)\left(\frac{m_1}{m_1+m_2}\right) \quad \ldots (3)$$

m_1 and m_2 are masses of the two satellites. B_1 and B_2 are the absolute values of the forces due to the direct solar pressure on m_1 and m_2 respectively and are small. Q_1 and Q_2 are the charges of the two satellites. μE is the magnitude of magnetic moment of the earth's dipole. p is the focal parameter. μ is the product of mass of the earth and gravitational constant. λ is undermined Lagrange's multiplier. ge is the force of gravity. e is ecentricity of the orbit of the centre of mass. v is the true anomaly of the centre of mass of the system. $\in$ is inclination of the oscillatory plane of the masses m_1 and m_2 with the orbital plane of the centre of mass of the system. α is the inclination of the ray. γ is a shadow function which depends on the illumination of the system of satellites by the sun rays. If γ is equal to zero, then the system is affected by the shadow of the earth. If γ is equal to one, then the system is not within the said shadow. R is the modulus of position vector of the centre of mass of the system. c_1 and c_2 are the Ballistic co-efficients. ρ_a is the average density of the atmosphere. i is inclination of the orbit with the equatorial plane. θ_2 is the angle between the axis of the cylindrical shadow beam and the line joining the centre of the earth and the end point of the orbit of the centre of mass within the earth's shadow, considering the positive direction towards the motion of the system. Prime denotes differentiation with respect to v.

If motion of one of the satellites m_1 be determined with the help of equations (1), motion of the other satellite of mass m_2 can be determined by Kumar[6]

$$m_1\overline{\rho_1} + m_2\overline{\rho_2} = 0 \quad \ldots (4)$$

where $\overline{\rho_j}\,(j = 1,2)$ is the radius vector in the centre of mass system.

For the analysis of the small secular and long periodic effects of the solar pressure and the effects of the earth's shadow on the system, the periodic terms in the equations of motion (1) may be averaged with respect to v as :

(*i*) From θ_2 to $(2\pi - \theta_2)$ for a period, when the system is under the influence of sun rays directly *i.e.* $\gamma = 1$ and

(*ii*) From $-\theta_2$ to $+\theta_2$ for a period, when the system is under the influence of shadow of the earth *i.e.* $\gamma = 0$.

The averaged values of the secular terms due to the periodic forces in the equations of motion (1) can be deduced as given below

$$\frac{1}{2\pi}\int_0^{2\pi}\frac{1}{\rho}dv = 1,\ \frac{1}{2\pi}\int_0^{2\pi}\rho dv = \frac{1}{\left(1-e^2\right)^{1/2}},\ \frac{1}{2\pi}\int_0^{2\pi}\frac{1}{\rho^2}dv = \left(1+\frac{1}{2}e^2\right)$$

$$\frac{1}{2\pi}\int_0^{2\pi}\rho^2 dv = \frac{1}{\left(1-e^2\right)^{3/2}},\ \frac{1}{2\pi}\int_0^{2\pi}\rho\rho' dv = 0$$

$$\frac{1}{2\pi}\int_0^{2\pi}\rho^3 dv = \frac{\left(2+e^2\right)}{2\left(1-e^2\right)^{5/2}},\ \frac{1}{2\pi}\int_0^{2\pi}\rho'\rho^{-2} dv = 0$$

$$\frac{1}{2\pi}\int_0^{2\pi}\rho^4 dv = \frac{\left(2+3e^2\right)}{2\left(1-e^2\right)^{7/2}},\ \frac{1}{2\pi}\int_0^{2\pi}\rho'\rho^{-1} dv = 0$$

$$\frac{1}{2\pi}\int_0^{2\pi}\gamma\left(\frac{B_1}{m_1}-\frac{B_2}{m_2}\right)\cos\in\cos\left(v-\alpha\right)dv = -\left(\frac{B_1}{m_1}-\frac{B_2}{m_2}\right)\frac{\cos\in\cos\alpha\sin\theta_2}{\pi}$$

and

$$\frac{1}{2\pi}\int_0^{2\pi}\gamma\left(\frac{B_1}{m_1}-\frac{B_2}{m_2}\right)\cos\in\sin\left(v-\alpha\right)dv = \left(\frac{B_1}{m_1}-\frac{B_2}{m_2}\right)\frac{\cos\in\sin\alpha\sin\theta_2}{\pi} \quad \ldots (5)$$

Using (5), equations (1) may be written as,

$$X''-2Y'-\frac{3X}{\left(1-e^2\right)^{1/2}} = \beta\frac{\left(2+3e^2\right)}{2\left(1-e^2\right)^{7/2}}X - A\cos i + \left(\frac{B_1}{m_1}-\frac{B_2}{m_2}\right)\frac{\cos\alpha\cos\in\sin\theta_2}{\pi}$$

and

$$Y''+2X' = \beta\frac{\left(2+3e^2\right)}{2\left(1-e^2\right)^{7/2}}Y + \left(\frac{B_1}{m_1}-\frac{B_2}{m_2}\right).\frac{\sin\alpha\cos\in\sin\theta_2}{\pi} - \frac{f}{\left(1-e^2\right)^{3/2}} \quad \ldots (6)$$

The condition of constraint given by (2) takes the form

$$X^2+Y^2\le\left(1+\frac{1}{2}e^2\right) \qquad \ldots (7)$$

Equations (6) do not contain the time explicity. Therefore, Jacobian integral of the problem must exist.

Multiplying the first and second equations of (6) by X' and Y' respectively and adding them we get,

$$X'X''+Y'Y''-\frac{3}{\left(1-e^2\right)^{1/2}}XX'=\beta\frac{\left(2+3e^2\right)}{2\left(1-e^2\right)^{7/2}}\left(XX'+YY'\right)-AX'\cos i+\left(\frac{B_1}{m_1}-\frac{B_2}{m_2}\right)$$

$$\text{x}\ .\frac{\cos\in\sin\theta_2}{\pi}\left(X'\cos\alpha+Y'\sin\alpha\right)-\frac{fY'}{\left(1-e^2\right)^{3/2}} \qquad \ldots (8)$$

Integrating (8) the expression comes as

$$X'^2+Y'^2-\frac{3}{\left(1-e^2\right)^{1/2}}X^2=\beta\frac{\left(2+3e^2\right)}{2\left(1-e^2\right)^{7/2}}\left(X^2+Y^2\right)-2AX\cos i+\frac{2}{\pi}\left(\frac{B_1}{m_1}-\frac{B_2}{m_2}\right)$$

$$\text{x}\ \cos\in\sin\theta_2\left(X\cos\alpha+Y\sin\alpha\right)-\frac{2fY}{\left(1-e^2\right)^{3/2}}+h \qquad \ldots(9)$$

Here h is the constant of integration which is known as Jacobian constant.

The surface of zero velocity can be obtained in the form

$$\frac{3}{\left(1-e^2\right)^{1/2}}X^2+\beta\frac{\left(2+3e^2\right)}{2\left(1-e^2\right)^{7/2}}\left(X^2+Y^2\right)-2AX\cos i+\frac{2}{\pi}\left(\frac{B_1}{m_1}-\frac{B_2}{m_2}\right)$$

$$\text{x}\ \cos\in\sin\theta_2\left(X\cos\alpha+Y\sin\alpha\right)-\frac{2fY}{\left(1-e^2\right)^{3/2}}+h=0 \qquad \ldots\ (10)$$

Thus it is concluded that the satellite m_1 moves inside the boundary of different curves of zero velocity represented by (12) for different values of the Jacobian constant.

3. Equilibrium solution of the problem

The equations of motion of the system in the rotating frame of reference have been obtained by (6). It is assumed that the system is moving with effective constraint and the connecting cable of the two satellites always remains tight.

The equilibrium positions of the system are given by the constant values of the co-ordinates in the rotating frame of reference.

Let $X = X_1$ = constant, $Y = Y_1$ constant … (11)

give the equilibrium positions, then

$$X' = X_1' = 0, \qquad Y' = Y_1' = 0$$
$$X'' = X_1'' = 0, \qquad Y'' = Y_1'' = 0 \quad \ldots (12)$$

Using (11) and (12) in the equations (6), we get,

$$\frac{3X_1}{\left(1-e^2\right)^{1/2}} + \frac{\beta}{2}\frac{\left(2+3e^2\right)}{\left(1-e^2\right)^{7/2}}X_1 = A\cos i - \left(\frac{B_1}{m_1} - \frac{B_2}{m_2}\right)\frac{\cos\in\cos\alpha\sin\theta_2}{\pi}$$

and

$$\frac{\beta}{2}\frac{\left(2+3e^2\right)}{\left(1-e^2\right)^{7/2}}Y_1 - \frac{f}{\left(1-e^2\right)^{3/2}} = -\left(\frac{B_1}{m_1} - \frac{B_2}{m_2}\right)\frac{\sin\alpha\cos\in\sin\theta_2}{\pi} \quad \ldots (13)$$

Actually, it is very difficult to obtain the solution of (13). Hence we are compelled to make our approaches with certain limitations. In addition to this, we are interested only to get the maximum effect of the earth's shadow on the motion of the system.

The presence of the perturbative term due to solar pressure clearly indicates that none of the coordinates of the libration point may be taken to be zero unless $\left(\frac{B_1}{m_1} - \frac{B_2}{m_2}\right)$ or $\theta_2 = 0$. But these parameters cannot be zero. In fact, $\in = 0$ will make the problem a particular case when the sun rays are in the orbital plane of the centre of mass of the system and also in the line of the perigee of the elliptical orbit.

Next, we put $\in = 0$ and $\alpha = 0$ in equations (13) and get,

$$\frac{3X_1}{\left(1-e^2\right)^{1/2}} + \frac{\beta}{2}\frac{\left(2+3e^2\right)}{\left(1-e^2\right)^{7/2}}X_1 = A\cos i - \left(\frac{B_1}{m_1} - \frac{B_2}{m_2}\right).\frac{\sin\theta_2}{\pi}$$

and

$$\frac{\beta}{2}\frac{\left(2+3e^2\right)}{\left(1-e^2\right)^{7/2}}Y_1 = \frac{f}{\left(1-e^2\right)^{3/2}} \qquad \ldots (14)$$

point as

$$[X_1, Y_1] = \left[\frac{A\cos i - \frac{1}{\pi}\left(\frac{B_1}{m_1} - \frac{B_2}{m_2}\right).\sin\theta_2}{\frac{\beta}{2}\frac{\left(2+3e^2\right)}{\left(1-e^2\right)^{7/2}} + \frac{3}{\left(1-e^2\right)^{1/2}}}, \frac{2f}{\beta}\frac{\left(1-e^2\right)^2}{\left(2+3e^2\right)}\right] \qquad \ldots (15)$$

4. Conclusion

In non-linear oscillation of the system, one equilibrium position exists when the perturbative forces like solar radiation pressure, shadow of the earth, earth's magnetic field and air resistance act on the system simultaneously. The equilibrium position has wide applications in solving problems of stability of a cable-connected satellites system in orbit. It will also state whether the motion of the system is continuous or not. The work may be further modified, if wobbling and nutation of the orbit of the system are taken into account.

Acknowledgements

I am thankful to UGC Kolkata for providing me the Research Project with Sanction Letter No. F. PSB-005/15-16, Dated 15.11.2016. I am also thankful to Prof. R. K. Sharma from Thiruvanathapuram for his encouragement.

References

1. Beletsky, V. V. and Novikova, E. T.− Kosmicheskie Issledovania , **7(6)**, pp. 377-384 (1969).
2. Beletsky, V. V. and Novoorebelskii, A. B.− Inst. of App. Maths., Acad. of Sci. of the U. S. S. R., **17**, pp. 213-219 (1969).
3. Das, S. K., Bhattacharya, P. K. and Singh, R. B.−Proc. Nat. Acad. Sci., India, **46**, pp. 287-299 (1976).
4. Kumar, S. and Bhattacharya, P. K.− Proc. Workshop on Spa. Dyn. and Cel. Mech., Muz., India, Eds. K. B. Bhatnagar and B. Ishwar, pp. 71-74 (1995).
5. Kumar, S., Srivastava, U. K. and Bhattacharya, P. K.−Proc. Math. Soc., B. H. U., Varanasi, **21**, pp. 51-61 (2005).
6. Kumar, S.−International Jour. in Phy. & Appl. Sci., **04 (Issue-07)**, pp. 01-11 (2017).
7. Singh, R. B. and Demin, V. G.−Cel. Mech., **06**, pp. 268-277 (1972).
8. Singh, R. B.−Astronau. Acta, **18**, pp. 301-308 (1973).
9. Nechvile, V. −Acad. Paris Compt. Rend., **182**, pp. 310-322 (1926).

INDIAN JOURNAL OF THEORETICAL PHYSICS, VOL. 65, NOS. 1 & 2, 2017

MHD visco-elastic fluid flow past a flat plate with heat and mass transfer

Bibhash Deka
Department of Mathematics, Gauhati University,
Guwahati-781014, Assam, India
E-mail: bibhashdeka66@gmail.com

and

Rita Choudhury
Department of Mathematics, Gauhati University,
Guwahati-781014, Assam, India
E-mail: rchoudhury66@yahoo.in

(Received for publication in May, 2017)

[Abstract : An analysis is carried out to study the boundary layer flow with heat and mass transfer which can be formed by an electrically conducting visco-elastic fluid past a flat plate in presence of magnetic field. The problem has been solved by the application of steepest descent method used by Meksyn. Analytical expressions for the velocity, temperature, concentration, shearing stress, Nusselt number and Sherwood number have been obtained and illustrated graphically to observe the effects of visco-elastic parameter with the combination of various values of pertinent flow parameters involved in the solution. The relevancy of this model has been noticed in various industrial and chemical processes.**]**

Key words: Visco-elastic, Boundary layer, Shearing stress, local heat flux, mass flux

1. Introduction

Newtonian flow characteristics are exhibited in most low molecular weight substances at constant temperature and pressure. But many substances of industrial significances do not conform to the Newtonian postulate. The anomalous or non-Newtonian behaviour occurs in a diverge range of applications, both in nature and technology.

In the theory of non-Newtonian fluid flow mechanics, the boundary layer concept is relevant to a number of engineering activities *viz*. manufacturing processes such as polymer extrusion, drawing of copper wires, hot rolling,

glass fiber, metal extrusion etc. Srivastava and Usha[1] have studied the laminar boundary layer on a moving continuous flat surface in presence of suction and magnetic field by using boundary value problem. The effect of magnetic field on laminar boundary layer flow on a flat plate has been investigated by Murthy and Sapre[2]. Meksyn[3] has used steepest descent method to find the value of arbitrary constants arising from the boundary condition at infinity in the case where the similarity solutions exist. Choudhury and Das[4] have examined the boundary layer flows of non-Newtonian fluid past a flat plate in presence of magnetic field. In this paper, we have analyzed the magnetohydrodynamic boundary layer visco-elastic fluid flow past a flat plate in presence of heat and mass transfer. Also, the authors *viz*. Chowdhury and Islam[5], Siddappa and Abel[6] , Damseh and Shannak[7], Vajravelu and Roper[8], Hayat, et. al.[9] Rajagopal and Gupta[10], Agarwal and Bhatia[11], Choudhury and Das[12] etc. have remarkable contribution in this field.

It is well known that non-Newtonian fluids behave differently under the action of stress imposed on them. As a result, different types of non-Newtonian fluids have emerged with different rheological properties to describe the dynamical behaviour of these fluids. The second-grade fluid model based on the postulate of gradually fading memory deduced by Coleman and Noll[13] is defined as

$$\sigma_{ij} = -p\delta_{ij} + \mu_1 A_{(1)ij} + \mu_2 A_{(2)ij} + \mu_3 A_{(1)ik} A_{(1)}{}^{\kappa}_{j} \quad \ldots \quad (1)$$

where σ_{ij} is the stress tensor, p is the indeterminate pressure and μ_1, μ_2 and μ_3 are material constants known as viscosity, elasticity and cross viscosity respectively. $A_{(i)}$ $(i = 1, 2)$ are the kinematic Rivlin-Ericksen tensors given by

$$A_{(1)ij} = v_{i,j} + v_{j,i} \quad \ldots \quad (2)$$

$$A_{(2)ij} = a_{i,j} + a_{j,i} + 2v_{m,i}v^{m}_{,j} \quad \ldots \quad (3)$$

where v_i and a_i are velocity and acceleration components respectively. Comma denotes covariant differentiation and are given by

$$a_i = \frac{Dv_i}{Dt} = \frac{\partial v_i}{\partial t} + v^m v_{i,m} \quad \ldots \quad (4)$$

It is noticed from thermodynamic consideration that the constants μ_1 and μ_3 are positive and μ_2 is negative [Coleman and Markovitz[14]]. It has already

been reported that the solution of polyisobutylene in cetane at 30^0C simulate a second-grade fluid and the material constants for the solutions of various concentrations have been determined by Markovitz. The present paper is concerned with the steady hydromagnetic flow of a semi-infinite expanse of an electrically conducting visco-elastic second-grade fluid bounded by an infinite rigid non-conducting plate with heat and mass transfer. The quantitative analysis is made to examine the influence of elasticity on the fluid velocity, temperature, concentration and also on the wall shear stress.

2. Mathematical formulation

We consider a steady incompressible two-dimensional flow of a visco-elastic fluid past a flat plate in presence of magnetic field of strength $B_y(x)$. The magnetic field acts in the transverse direction of the plate. In case of large transverse magnetic field and small electric conductivity, the two-dimensional boundary layer equations are given as follows :

$$\frac{\partial u}{\partial x}+\frac{\partial v}{\partial y}=0 \qquad \ldots \quad (5)$$

$$u\frac{\partial u}{\partial x}+v\frac{\partial u}{\partial y}=U\frac{\partial U}{\partial x}+\nu_1\frac{\partial^2 u}{\partial y^2}+\nu_2\left\{\frac{\partial u}{\partial x}\frac{\partial^2 u}{\partial y^2}+u\frac{\partial^3 u}{\partial x\partial y^2}+v\frac{\partial^3 u}{\partial y^3}+\frac{\partial u}{\partial y}\frac{\partial^2 v}{\partial y^2}\right\}$$

$$+\frac{\sigma^* {B_y}^2}{\rho}(U-u) \qquad \ldots \quad (6)$$

$$\rho c_p\left(u\frac{\partial T}{\partial x}+v\frac{\partial T}{\partial y}\right)=k\frac{\partial^2 T}{\partial y^2}+\mu_1\left(\frac{\partial u}{\partial y}\right)^2+\mu_2\left(u\frac{\partial u}{\partial y}\frac{\partial^2 u}{\partial x\partial y}+v\frac{\partial u}{\partial y}\frac{\partial^2 u}{\partial y^2}\right) \quad \ldots \quad (7)$$

$$u\frac{\partial C}{\partial x}+v\frac{\partial C}{\partial y}=D_m\frac{\partial^2 C}{\partial y^2} \qquad \ldots \quad (8)$$

The boundary conditions on u, v, T and C are given as follows :

$$u=0, v=0, T=T_w, C=C_w \text{ at } y=0 \qquad \ldots \quad (9)$$

$$u\to U, T\to T_\infty, C\to C_\infty \text{ as } y\to\infty \qquad \ldots \quad (10)$$

where $y\to\infty$ denotes the edge of the boundary layer and U is constant potential flow velocity. Here x is the co-ordinate measured along the surface from the slit location in the direction of its motion, y is the co-ordinate normal to the surface, u and v are the velocity components along x and y axes respectively, ρ is the fluid density, σ^* is the electric conductivity, C_p is

the specific heat, k is the thermal conductivity, T is dimensional temperature, C is dimensional species concentration and D_m is the co-efficient of chemical molecular diffusivity (Fig. 1).

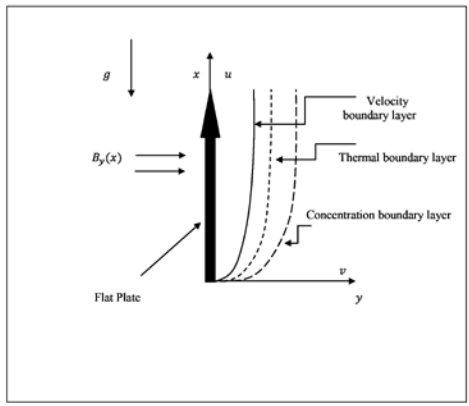

Fig. 1
Physical model and co-ordinate system.

We consider a stream function ψ (x, y) such that $u = \frac{\partial \psi}{\partial y}, v = -\frac{\partial \psi}{\partial x}$ which satisfies the equation (5). we set $\vartheta_{21}(x) = \vartheta_{22}x^{\varepsilon}$, $S(x) = S_0 x^{\varepsilon}$, $G(\eta) = \frac{T-T_\infty}{T_w-T_\infty}$, $H(\eta) = \frac{C-C_\infty}{C_w-C_\infty}$ and put $\eta = (\frac{U}{2\nu_1 x})^{1/2} y$, $\psi = (2\nu_1 U x)^{\frac{1}{2}} f(\eta)$, $Sc = \frac{\nu_1}{D_m}$, $Pr = \frac{\rho c_p \nu_1}{k}, E = \frac{U^2}{c_p(T_w-T_\infty)}$. Then the transformed forms of equations (6) to (8) are given by,

$$f''' + ff'' = M(f' - 1) + \alpha_1(2f'f''' + ff'''' - f''^2) \quad \ldots \quad (11)$$

$$G'' + PrfG' = PrE\{\alpha_1(f'f''^2 + ff''f''') - f''^2\} \quad \ldots \quad (12)$$

$$H'' + ScfH' = 0 \quad \ldots \quad (13)$$

where $M = \frac{2S_0}{U}, \alpha_1 = \frac{\vartheta_{22}U}{2\nu_1}$

The corresponding boundary conditions are:

$$f(0) = 0, f'(0) = 0, G(0) = 1, H(0) = 1 \text{at } \eta = 0 \quad \ldots \quad (14)$$

$$f'(\eta) \to 1, G(\eta) \to 0, H(\eta) \to 0 \text{ as } \eta \to \infty \quad \ldots \quad (15)$$

where f is the non-dimensional stream function, η is the transformed co-ordinate, M is the magnetic parameter, α_1 is the visco-elastic parameter, G is the dimensionless temperature, H is the dimensionless species concentration, Sc is the Schmidt number, Pr is the prandtl number, E is the Eckert number.

3. Method of solution

The equations (11) to (13) subject to the boundary conditions (14) and (15) can be solved by any numerical method but we have solved these equations by the method of series expansion followed by the Laplace transform method. For this purpose, we express the functions (η), $G(\eta)$ and $H(\eta)$ in power series of η as,

$$f(\eta) = \frac{a_2}{2!}\eta^2 + \frac{a_3}{3!}\eta^3 + \frac{a_4}{4!}\eta^4 + \frac{a_5}{5!}\eta^5 + \frac{a_6}{6!}\eta^6 + \frac{a_7}{7!}\eta^7 + \cdots \quad \ldots \quad (16)$$

$$G(\eta) = 1 + b_1\eta + \frac{b_2}{2!}\eta^2 + \frac{b_3}{3!}\eta^3 + \frac{b_4}{4!}\eta^4 + \frac{b_5}{5!}\eta^5 + \cdots \quad \ldots \quad (17)$$

$$H(\eta) = 1 + c_1\eta + \frac{c_2}{2!}\eta^2 + \frac{c_3}{3!}\eta^3 + \frac{c_4}{4!}\eta^4 + \frac{c_5}{5!}\eta^5 + \cdots \quad \ldots \quad (18)$$

The forms (16) to (18) of (η), $G(\eta)$ and $H(\eta)$ respectively satisfy the boundary conditions (14). Substituting the expressions of $f(\eta)$, $G(\eta)$ and $H(\eta)$ from (16) to (18) in the equations (11) to (13) and equating the co-efficients of different powers of $f\eta$ to zero, we obtain the constants a_i, b_j and C_k (i = 2, 3, 4….; j = 1, 2, 3…..; k = 1, 2, 3…..) as follows :

$$a_3 = -\left(M + \alpha_1 a_2^{\,2}\right),$$

$$a_4 = M\, a_2,$$

$$a_5 = \left\{a_2^{\,2}\left(2\alpha_1 M - 1\right) - M^2\right\},$$

$$a_6 = \left\{a_2 M^2 + \alpha_1 a_2^{\,3}\left(11\alpha_1 M - 3\right) - 10\alpha_1 M^2 a_2 + 4a_2 M\right\},$$

$$a_7 = \left\{38\alpha_1 M a_2^{\,2} + 112\alpha_1^{\,3} M a_2^{\,4} - 30\alpha_1^{\,2} a_2^{\,4} - 8M a_2^{\,2} + M^2 \left(17\alpha_1 a_2^{\,2} - M - 4 - 130\alpha_1^{\,2} a_2^{\,2} + 10\alpha_1 M\right)\right\},$$

$$b_2 = -Pr\, E a_2^{\,2},$$

$$b_3 = Pr\, E\left(3a_2^{\,2}\alpha_1 + 2Ma_2\right),$$

$$b_4 = \left\{Pr\, E\left(-8\alpha_1^{\,2} a_2^{\,4} - 10\alpha_1 M a_2^{\,2} - M a_2^{\,2} - 2Ma^2\right) - Pr\, a_2 b_1\right\},$$

$$b_5 = \left\{ Pr\,E\left(13\alpha_1 a_2 a_3^2 + 6a_4 a_2^2 - a_2 a_5 - 6a_3 a_4\right) - Pr\left(a_3 b_1 + 3a_2 b_2\right)\right\}, \ldots\ldots\ldots$$

$$C_2 = 0,$$

$$C_3 = 0,$$

$$C_4 = -a_2 c_1 Sc,$$

$$C_5 = Sc\left(\alpha_1 a_2{}^2 + M\right)c_1, \ldots\ldots\ldots$$

We use steepest descent method used by Meksyn and determine the constants a_i, b_j and c_k. Accordingly the velocity, temperature and concentration distributions are completely determined. To obtain the values of a_i, b_j and c_k, we will first determine the values of a_2, b_1 and c_1. We write the equations (11) and (12) in the following forms,

$$f''' + ff'' = L(\eta) \quad \ldots \quad (19)$$

$$G'' + PrfG' = R(\eta) \quad \ldots \quad (20)$$

where $L(\eta)$ and $R(\eta)$ are the right hand sides of equations (11) and (12) respectively. Now, integrating twice the equations (19), (20) and (13), we get,

$$f'(\eta) = \int_0^\eta e^{-I(\eta)}\,\lambda(\eta)d\eta \quad \ldots \quad (21)$$

$$G(\eta) = 1 + \int_0^\eta e^{-J(\eta)}\,\theta(\eta)d\eta \quad \ldots \quad (22)$$

$$H(\eta) = 1 + c_1 \int_0^\eta e^{-K(\eta)}\,d\eta \quad \ldots \quad (23)$$

where,

$$I(\eta) = \int_0^\eta f(\eta)d\eta$$

$$J(\eta) = Pr \int_0^\eta f(\eta)d\eta$$

$$K(\eta) = Sc \int_0^\eta f(\eta)d\eta$$

$$\lambda(\eta) = a_2 + \int_0^\eta e^{I(\eta)}\,L(\eta)d\eta$$

$$\theta(\eta) = b_1 + \int_0^\eta e^{J(\eta)}\,R(\eta)d\eta$$

Now, taking $\eta \to \infty$ in the equations (21) to (23), we get,

$$\int_0^\infty e^{-I(\eta)}\,\lambda(\eta)d\eta = 1 \quad \ldots \quad (24)$$

$$\int_0^\infty e^{-J(\eta)}\,\theta(\eta)d\eta = -1 \quad \ldots \quad (25)$$

$$c_1\int_0^\infty e^{-K(\eta)}\,d\eta = -1 \quad \ldots \quad (26)$$

These integrals can be evaluated asymptotically by Laplace's method. Putting $I = J = K = \zeta$, transforming the equations (24) to (26) to the variable ζ and integrating in the gamma functions, we find

$$1 = r_{00}\Gamma_{\frac{1}{3}} + r_{01}\Gamma_{\frac{2}{3}} + r_{02}\Gamma_1 + r_{03}\Gamma_{\frac{4}{3}} + r_{04}\Gamma_{\frac{5}{3}} + \cdots \quad \ldots \quad (27)$$

$$-1 = r_{10}\Gamma_{\frac{1}{3}} + r_{11}\Gamma_{\frac{2}{3}} + r_{12}\Gamma_1 + r_{13}\Gamma_{\frac{4}{3}} + r_{14}\Gamma_{\frac{5}{3}} + \cdots \quad \ldots \quad (28)$$

$$-1 = r_{20}\Gamma_{\frac{1}{3}} + r_{21}\Gamma_{\frac{2}{3}} + r_{22}\Gamma_1 + r_{23}\Gamma_{\frac{4}{3}} + r_{24}\Gamma_{\frac{5}{3}} + \cdots \quad \ldots \quad (29)$$

where the constants $(r_{00}, r_{01}, \ldots r_{10}, r_{11}, \ldots r_{20}, r_{21}, \ldots.)$ are not presented here due to sake of brevity. Now solving equations (27) to (29) using MATLAB software, the values of a_2, b_1 and c_1 have been determined for different values of α_1, M, Pr and Sc. The Eckert number is taken fixed at E=0.001. After knowing the values of a_2, b_1 and c_1, we can easily find the values of a_3, a_4, a_5, ….. b_2, b_3, b_4, …… c_2, c_3, c_4, ……. etc. Now using these values in equations (16) to (18), we get the expressions for $f(\eta)$, $G(\eta)$, and $H(\eta)$ respectively as,

$$\begin{aligned} f(\eta) = {} & \tfrac{1}{2!}\eta^2 a_2 - \tfrac{1}{3!}\eta^3(M + \alpha_1 {a_2}^2) + \tfrac{1}{4!}\eta^4 M a_2 + \tfrac{1}{5!}\eta^5\{{a_2}^2(2\alpha_1 M - 1) - M^2\} \\ & + \tfrac{1}{6!}\eta^6\{a_2 M^2 + \alpha_1 {a_2}^3(11\alpha_1 M - 3) - 10\alpha_1 M^2 a_2 + 4a_2 M\} + \tfrac{1}{7!}\eta^7 \\ & \{38\alpha_1 M {a_2}^2 + 112{\alpha_1}^3 M {a_2}^4 - 30{\alpha_1}^2 {a_2}^4 - 8M{a_2}^2 + \\ & M^2(17\alpha_1 {a_2}^2 - M - 4 - 130{\alpha_1}^2 {a_2}^2 + 10\alpha_1 M)\} + \ldots\ldots \end{aligned} \quad \ldots \quad (30)$$

$$\begin{aligned} G(\eta) = {} & 1 + b_1\eta - \tfrac{1}{2!}\eta^2 PrE{a_2}^2 + \tfrac{1}{3!}\eta^3 PrE(3{a_2}^3\alpha_1 + 2Ma_2) + \tfrac{1}{4!}\eta^4\{PrE(-8{\alpha_1}^2{a_2}^4 - \\ & 10\alpha_1 M{a_2}^2 - M{a_2}^2 - 2M^2) - Pra_2 b_1\} + \tfrac{1}{5!}\eta^5\{PrE(13\alpha_1 a_2 a_3^2 + 6a_4 a_2^2 \cdot \\ & - a_2 a_5 - 6a_3 a_4)\, Pr(a_3 b_1 + 3a_2 b_2)\} + \ldots\ldots \end{aligned} \quad \ldots \quad (31)$$

$$H(\eta) = 1 + c_1\eta - \tfrac{1}{4!}\eta^4 a_2 c_1 Sc + \tfrac{1}{5!}\eta^5 Sc(\alpha_1 {a_2}^2 + M)c_1 + \ldots\ldots \quad \ldots \quad (32)$$

and the velocity components along xes are given by,

$$u = Uf'(\eta) \quad \ldots \quad (33)$$

$$v = \left(\frac{U\nu_1}{2x}\right)^{\frac{1}{2}}\{\eta f'(\eta) - f(\eta)\} \quad \ldots \quad (34)$$

4. Results and discussion

Knowing the velocity, temperature and concentration fields, we obtain some important flow characteristics of the problem *viz*. wall shear stress, local heat flux and mass flux.

The non-dimensional shearing stress τ at the plate $\eta = 0$ is given by,

$$\tau = \frac{\sigma_{xy}}{\rho U\left(\frac{U\nu_1}{2x}\right)^{\frac{1}{2}}} = \frac{d^2 f}{d\eta^2}\Big]_{\eta=0} \quad \ldots \quad (35)$$

The non-dimensional heat flux at the plate $\eta = 0$, in terms of Nusselt number Nu is given by,

$$Nu = \frac{dG}{d\eta}\Big]_{\eta=0} \quad \ldots \quad (36)$$

The non-dimensional mass flux at the plate $\eta = 0$, in terms of Sherwood number Sh is given by,

$$Sh = \frac{dH}{d\eta}\Big]_{\eta=0} \quad \ldots \quad (37)$$

To get the physical insight of the problem, the numerical computations have been carried out for velocity, temperature and concentration fields. Throughout the computations, we employ different values of the visco-elastic parameter α_1, magnetic parameter M, Prandtl number Pr and Schmidt number Sc. Visco-elastic fluid is characterized by the non-zero values of α_1 and $\alpha_1 = 0$ represents the character of Newtonian fluid flow phenomenon.

Figures 2 and 3 demonstrate the variation of the velocity $f'(\eta)$ against with different values of magnetic parameter M. In each of the graphs, the fluid velocity enhances considerably away from the plate for both Newtonian and visco-elastic (non-Newtonian) fluids. With the growth of the absolute value of the visco-elastic parameter α_1 ($\alpha_1 = 0, -0.2, -0.4$), the fluid velocity accelerates in comparison with Newtonian fluid flow phenomenon. Also, the fluid velocity decelerates with the growth of magnetic parameter M for both simple and visco-elastic fluid flow regions. This shows conformity with the fact that the effect of magnetic field on an electrically

conducting fluid gives rise to a resistive type force known as Lorentz force which has tendency to slow down the motion of the fluid.

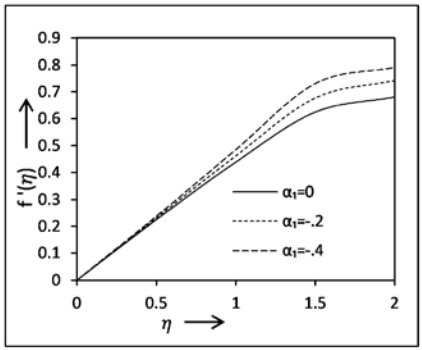

Fig. 2
Variation of $f(\eta)$ against η for $M = 0.02$.

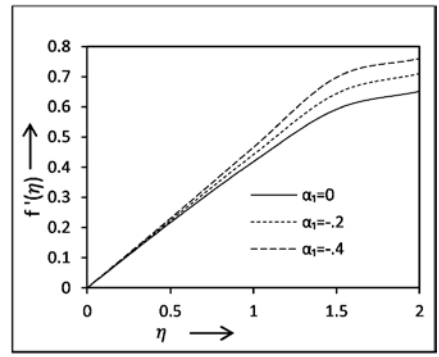

Fig. 3
Variation of $f(\eta)$ against η for $M = 0.04$.

Figures 4 and 5 examine the variation of the temperature $G(\eta)$ against η with various values of other flow parameters. The graphs reveal that the temperature gradually diminishes away from the plate for both types of fluids. Also, the temperature of the fluid significantly slows down with the rise of Prandtl number.

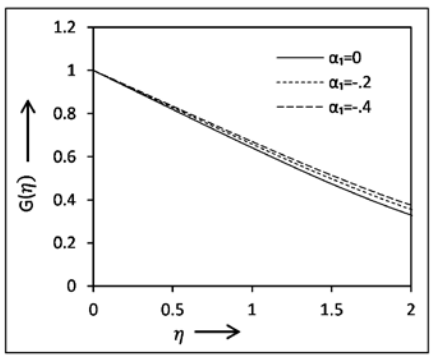

Fig. 4
Variation of $G(\eta)$ against η for $M = 0.02$ $Pr = 0.5$ and $E = 0.001$.

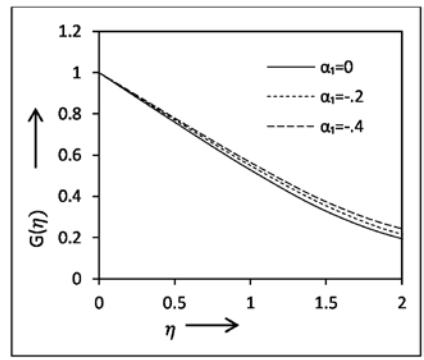

Fig. 5
Variation of $G(\eta)$ against η for $M = 0.02$ $Pr = 1.1$ and $E = 0.001$.

The variation of the concentration $H(\eta)$ against is illustrated by the figures 6 and 7. The figures depict that the concentration of the fluid gradually diminishes away from the plate for both Newtonian and visco-elastic fluids. Again, when the mass diffusivity is less than that of the

kinematic viscosity then the decelerating nature of the concentration profile is also noticed.

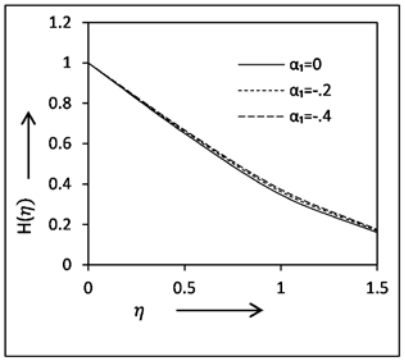

Fig. 6
Variation of $H(\eta)$ against η for $M = 0.02$ and $Sc = 2$.

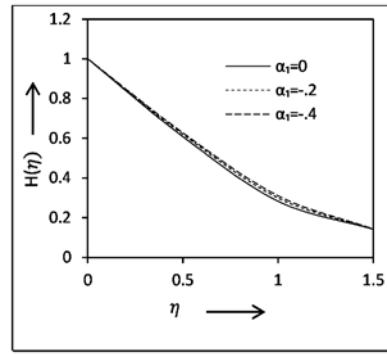

Fig. 7
Variation of $H(\eta)$ against η for $M = 0.02$ and $Sc = 3$.

It is very important to know the effect of visco-elasticity on resistive force or viscous drag and consequently the shearing stress. The shearing stress τ against the magnetic parameter M is depicted by the Fig. 8. The rise of the absolute value of the visco-elasticity enhances the shearing stress in comparison with the simple flow fluid.

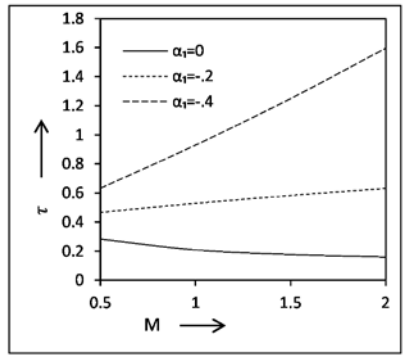

Fig. 8
Variation of τ against M.

Figures 9 and 10 represent the variations of Nusselt number Nu against M and Pr respectively. With the growth of absolute value of visco-elastic parameter α_1, the Nusselt number decreases against the magnetic parameter M (Fig. 9) but an opposite behaviour in Nusselt number is experienced in

case of Prandtl number *Pr* (Fig. 10). Similar results are noticed in case of Sherwood number. The Sherwood number *Sh* diminishes gradually with the enhancement of the magnetic parameter *M* (Fig. 11) but an opposite trend is found when it varies against Schmidt Number *Sc* (Fig. 12).

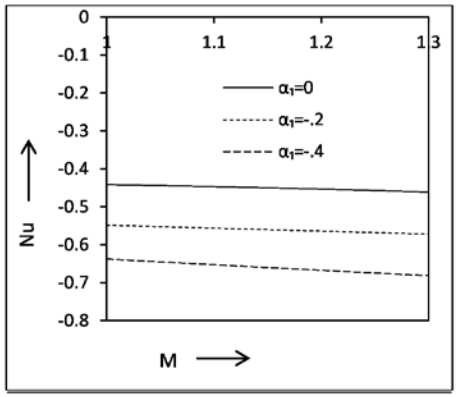

Fig. 9
Variation of *Nu* against *M* for *Pr* = 1.1 and *E* = 0.001.

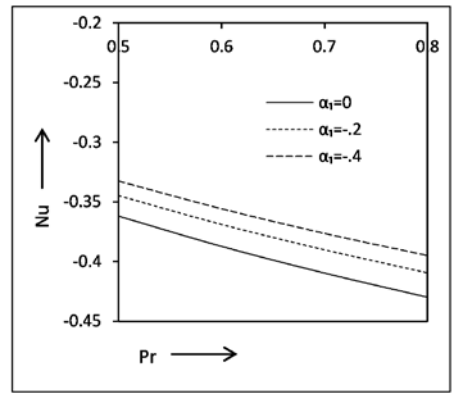

Fig. 10
Variation of *Nu* against *Pr* for *M* = 0.02 and *E* = 0.001.

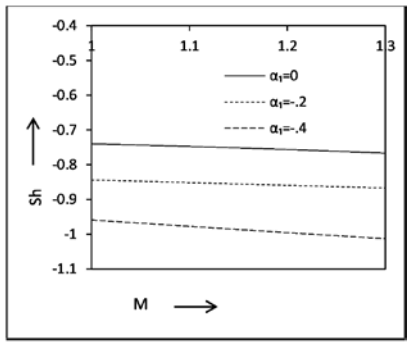

Fig. 11
Variation of *Sh* against *M* for *Sc* = 3.

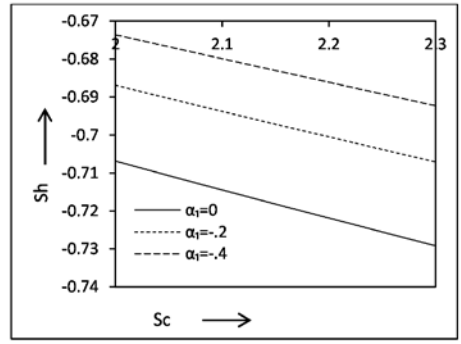

Fig. 12
Variation of *Sh* against *Sc* for *M* = 0.02.

5. Conclusion

The study leads to the following conclusions:

- The velocity field is significantly affected at each point of the fluid flow region by the visco-elastic parameter.
- The enhancement of magnetic parameter diminishes the fluid velocity and this shows conformity with physical behaviour of magnetic parameter.

- The temperature and concentration fields are affected noticeably by visco-elasticity.
- The variation of shearing stress in the fluid flow region against the pertinent flow parameter in presence of visco-elasticity is considerable.
- The Nusselt number and Sherwood number play vital roles in flow characteristics. The effect of visco-elasticity is significant in both the cases.

Acknowledgement

The financial support by UGC in the form MRP-Major-2013-8485 General (NER), F.No.-43-416/2014 (SR) dated 1st September 2015 is gratefully acknowledged by the authors**.**

References

1. Shrivastava, U.N. and Usha, S.– Magneto-fluid dynamic boundary layer on a moving continuous flat surface, Indian J. pure Appl. Math., **18**(9), 741-751, (1987).
2. Murthy, S.N. and Sapre, M.– Effect of magnetic field on laminar boundary layer flow on a flat plate, Indian J. pure Appl. Math., **22**(7), 601-609, (1991).
3. Meksyn, D.– New Method in Laminar Boundary layer theory, Pergamon Press (1961).
4. Choudhury, R. and Das, A.– Magneto-Hydrodynamic boundary layer flows of non-Newtonian fluid past a flat plate, Indian J. pure Appl. Math., **31**(11), 1429-1441, (2000).
5. Chowdhury, M. K. and Islam, M.N.– MHD free convection flow of visco-elastic fluid past an infinite vertical porous plate, Heat and Mass Transfer, **36**(5), 439-447, (2000).
6. Siddappa, B. and Abel, M.S.– Visco-elastic boundary layer flow past a stretching plate with suction and heat transfer, Rheologica Acta , **25**(3), 319–320, (1986).
7. Damseh, R.A. and Shannak, B.A. – Visco-elastic fluid flow past an infinite vertical porous plate in the presence of first-order chemical reaction, Appl. Math. and Mech., **31**(8), 955-962, (2010).
8. Vajravelu, K. and Roper,T.– Flow and heat transfer in a second grade fluid over a stretching sheet, Int. J. non-linear Mech., **34**(6), 1031-1036, (1999).
9. Hayat,T., Abbas, Q., Asghar, S., Siddique, A.M. and Murtaza, G.– Flow of an elastic-viscous fluid past an infinite wall with time dependent suction , Acta Mech., **153**, 133-145, (2002).

10. Rajagopal, K.R. and Gupta, A.S.– An exact solution for the flow of an non-Newtonian fluid past an infinite plate on boundary conditions for fluids of differential type, Meccanica, **19**, 158-160, (1984).
11. Agarwal, R.S. and Bhatia, S.P.S.– Heat transfer in second-order fluid with suction and constant heat sources, Int. J. Phys., **47,** 423-431, (1973).
12. Choudhury, R. and Das, U. J. –Visco-elastic effects on the three-dimensional hydrodynamic flow past a vertical porous plate, Int. J. Heat and Technology, **31**, 1-8, (2013).
13. Coleman, B.D. and Noll, W. – An application theorem for functional with applications in continuum mechanics, Archs Ration Mech. Analysis, **6,** 350-360, (1960).
14. Coleman, B.D. and Markovitz, H. – Incompressible second-order fluids, Adv. Appl. Mech., **8**, 69-101, (1964).

INDIAN JOURNAL OF THEORETICAL PHYSICS, VOL. 65, NOS. 1 & 2, 2017

A note on the decay of homogeneous isotropic temperature fluctuations field by Smirnov and Shapiro method

S. K. Saha*
M. C. Chaki Centre for Mathematics and
Mathematical Sciences, Kolkata-25
E-mail: sksaha30@gmail.com

and

H. P. Mazumdar
Honorary Visiting Professor, Indian Statistical Institute,
Kolkata-700108, India
E-mail: hpmi2003@yahoo.com

(Received for publication in May, 2017)

[Abstract: In this paper, we investigate the well known method due to Smirnov and Shapiro[11] to solve the differential equations pertaining to homogeneous and isotropic fluctuations field for the velocity and temperature. It is shown here that the use of Smirnov and Shapiro method is more instructing than the Millionschikov's closure hypothesis as applied to homogeneous isotropic turbulence.]

Key words : Homogeneous isotropic temperature fluctuations field, Smirnov and Shapiro method.

1. Introduction

In his text, Random function and turbulence Panchev[1] discussed several additional problems of statistical theory of turbulence and their applications. Karman and Howarth [2] established first the dynamical equation

$$(\frac{\partial}{\partial t} - 2\nu D_5)B_{ll} = (\frac{\partial}{\partial r} + \frac{4}{r})B_{lll}, \qquad \dots \quad (1)$$

where clearly, it determines the change $B_{ll}(r, t)$ in time and consequently describe the decay process of turbulence, B_{ll} , B_{lll} are respectively the two points double and triple correlations. Karman and Howarth[2] introduced the

* Mailing Address : 28/348, Kumar Lane, Chinsurah, Hooghly-712101, W.B., India

hypothesis of the similarity of correlation fluctuations in the process of decay and which they expressed mathematically, as

$$B_{ll}(r, t) = \sigma_u^2 \, f(\frac{r}{L}) \text{ and} \quad \ldots \quad (2)$$

$$B_{lll}(r, t) = \sigma_u^2 \, h(\frac{r}{L}), \quad \ldots \quad (3)$$

where L is a certain linear scale. Loitzianskii[3] introduced an invariant integral form *e.g.*

$$\Lambda = \int_0^\infty r^4 B_{ll}(r, t) dr, \quad \ldots \quad (4)$$

and expressed by means of the indicated hypothesis in the form

$$\sigma_u^2 \, L^5 = \text{constant}. \quad \ldots \quad (5)$$

As in the initial stage, the influence of friction is unsubstantial and the rate of diffusion of energy $\frac{d\sigma_u^2}{dt}$ depends only upon σ_u and L, that is, $\frac{d\sigma_u^2}{dt} \sim \frac{\sigma_u^3}{L}$, we can put $\sigma_u^2(t) \sim t^{-\frac{10}{7}}$, $L(t) \sim t^{\frac{2}{7}}$.

These decay laws were established by Kolmogrov[1].

The inherent closure problem of turbulence has been tackled by computing Millionstchikov's original hypothesis[4] that at the final stage of decay of isotropic turbulence, the joint probability distributions of the values of velocity at two different points but at one and the same instant of time are near to the normal distribution so that the relationship between fourth and second order moments is approximately correct, the third order moment accordingly differs from zero (see Panchev[1], Chandasekhar[5,6]) discussed elaborately about the components of velocity in the product $\overline{u_i u_j u'_k u'_m}$ that are taken at two points and at two different instants of time. At this stage a generalization of the above hypothesis was proposed so that it can be applied to mixed moments of fourth order constructed from scalar and vector quantities, only scalar or only vector quantities relating to one and the same or different instant of time to one and the same or different points. Chandrashekhar[5,7] formulated a proficient theory for the stationary, homogeneous and isotropic turbulence. In fact Chandrashakar[5] constructed a pair of non-linear differential equations and these equations are solved by the help of Millionschikov's quasi normality hypothesis.

In the next section we write down a pair of differential equations and solve the original system for the turbulence case, especially, for the mixed moment cases, namely, velocity fields, the scalar fields and temperature fields or concentration fields or reactant concentration fields etc. by employing Millionschikov's quasi normality hypothesis. In such hypothesis we generally use three dimensional single valued series solution and work out the complete solution of turbulence, taking a particular, the generalized moment method as discussed earlier.

2. Solution of a pair of differential equations

In this section we solve the following differential equation for isotropic temperature fluctuations in isotropic turbulence:

The basic equation (4) giving the temperature correlation function m in terms of Q, where Q is the defining scalar of second order isotropic tensor[5] Q_{ij} is

$$[\pm\frac{\partial}{\partial t} - \gamma\nabla^2]^2 \, m\overline{\theta^2} = \frac{2}{r^2}\frac{\partial}{\partial r}[\, Qr^2 \frac{\partial m\overline{\theta^2}}{\partial r}], \qquad \ldots \quad (6)$$

where θ is the temperature fluctuation at the point r and at time t and $\nabla^2 = \frac{\partial^2}{\partial r^2} + \frac{2}{r}\frac{\partial}{\partial r}$.

The equation giving the values[5] of Q is

$$\frac{\partial}{\partial r}[\frac{\partial^2}{\partial t^2} - v^2 D_5^2 \,]Q = -\, 2Q\frac{\partial}{\partial r} D_5 Q, \qquad \ldots \quad (7)$$

where

$$D_n = \frac{\partial^2}{\partial r^2} + \frac{n-1}{r}\frac{\partial}{\partial r}. \qquad \ldots \quad (8)$$

For extremely large Pleclet number $\gamma \to 0$ and (6) reduces to

$$\frac{\partial^2 (m\overline{\theta^2})}{\partial t^2} = \frac{2}{r^2}\frac{\partial}{\partial r}[\, Qr^2 \frac{\partial m\overline{\theta^2}}{\partial r}]. \qquad \ldots \quad (9)$$

Let

$$m(r, t) = \frac{m_1}{<\theta^2>} \text{ and } f(r, t) = \frac{Q}{<u^2>}. \qquad \ldots \quad (10)$$

From (9) and (10) we get

$$\frac{\partial^2 m_1}{\partial t^2} = < u^2 > [\frac{4}{r} f\frac{\partial m_1}{\partial r} + 2\frac{\partial f}{\partial r}\frac{\partial m_1}{\partial r} + 2f\frac{\partial^2 m_1}{\partial r^2}\,]. \qquad \ldots \quad (11)$$

From (7) and (10) we get

$$\frac{\partial}{\partial r}[\frac{\partial^2}{\partial t^2} - v^2 D_5^2]f = -2 < u^2 > f \frac{\partial}{\partial r} D_5 f. \quad \ldots \quad (12)$$

Since m_1 and f are even functions of r and t, therefore we may take the following power series for m_1 and f:

$$m_1 = \sum_{i=0}^{\infty} \sum_{k=0}^{\infty} a_{i,k} r^{2i} t^{2k} \ (a_{0,0} = 1), \quad \ldots \quad (13)$$

$$f = \sum_{i=0}^{\infty} \sum_{k=0}^{\infty} b_{i,k} r^{2i} t^{2k} \ (b_{0,0} = 1). \quad \ldots \quad (14)$$

Putting (13) and (14) in (11) we get

$$\sum_{i=0}^{\infty} \sum_{k=1}^{\infty} 2k(2k-1)\, a_{i,k} r^{2i} t^{2k-2}$$

$$= < u^2 > [\frac{4}{r} \sum_{i=1}^{\infty} \sum_{k=o}^{\infty} \sum_{l=0}^{\infty} \sum_{m=0}^{\infty} 2i a_{i.k}\, b_{l,m}\, r^{2i+2l-1}\, t^{2k+2m}$$

$$+ 2 \sum_{i=1}^{\infty} \sum_{k=o}^{\infty} \sum_{l=1}^{\infty} \sum_{m=0}^{\infty} 2i2l a_{i.k}\, b_{l,m}\, r^{2i+2l-2}\, t^{2k+2m}$$

$$2 \sum_{i=1}^{\infty} \sum_{k=o}^{\infty} \sum_{l=0}^{\infty} \sum_{m=0}^{\infty} 2i(2i-1) a_{i.k}\, b_{l,m}\, r^{2i+2l-2}\, t^{2k+2m}] \quad \ldots \quad (15)$$

Equating the coefficients of $r^{2i} t^{2k}$ from the both sides of (15), we obtain

$$a_{i,k+1} = \frac{1}{(k+1)(2k+1)} [< u^2 > \sum_{p=0}^{i} \sum_{q=0}^{k} (i-p)(2i+3)\, a_{i-p,k-q} b_{p+1,,q}]. \quad (16)$$

Again putting (14) in (12) we get

$$\sum_{i=1}^{\infty} \sum_{k=1}^{\infty} 4ik(2k-1) b_{i,k}\, r^{2i-1} t^{2k-2} -$$

$$- v^2 \sum_{i=3}^{\infty} \sum_{k=0}^{\infty} 8i(i-1)(i-2)(2i+1)(2i+3)\, b_{i,k} r^{2i-5}\, t^{2k} \quad \ldots \quad (17)$$

$$= -2 < u^2 > \sum_{i=0}^{\infty} \sum_{k=o}^{\infty} \sum_{l=2}^{\infty} \sum_{m=0}^{\infty} 4l(l-1)(2l+3) b_{i.k}\, b_{l,m}\, r^{2i+2l-3}\, t^{2k+2m}.$$

Equating the coefficient of $r^{2i+1} t^{2k}$ from the both sides of (17) we obtain

$$b_{i+1,k+1} = \frac{1}{(i+1)(k+1)(2k+1)} [\, 2v^2 (i+1)(i+2)(i+3)(2i+7)(2i+9 b_{i+3,k})$$

$$- 2 < u^2 > \sum_{p=0}^{i} \sum_{q=0}^{k} (p+1)(p+2)\,(2p+7)\, b_{i-p,k-q} b_{p+2,q}]. \quad \ldots \quad (18)$$

Since the correlation decreases with the distance, it may be assumed that

$$[\frac{\partial^2}{\partial t^2} - v^2 D_5^2]f(r, t) = 0. \quad \ldots \quad (19)$$

Integrating (12) with respect to r, we get

$$[\frac{\partial^2}{\partial t^2} - v^2 D_5^2]\,f(r,t) = -2\langle u^2\rangle \int_0^r f(r',t)\frac{\partial}{\partial r'} D_5 f(r',t)dr' + 2\langle u^2\rangle c(t), \quad \ldots (20)$$

where $c(t)$ is a constant and contains the terms involving t.

Making $r\to\infty$ and using the equation (19) we obtain

$$\int_0^\infty f(r',t)\frac{\partial}{\partial r'} D_5 f(r',t)dr' = c(t) = \sum_{k=0}^\infty c_k\, t^{2k} \text{ (say)}. \quad \ldots (21)$$

Substituting (14) in (20) we get

$$\sum_{i=0}^\infty \sum_{k=1}^\infty 2k(2k-1)\, b_{i,k} r^{2i} t^{2k-2} - v^2 \sum_{i=2}^\infty \sum_{k=0}^\infty 4i(i-1)(2i+1)(2i+3)\, b_{i,k} r^{2i-4}\, t^{2k} = 2\langle u^2\rangle \sum_{k=0}^\infty c_k\, t^{2k}. \quad \ldots (22)$$

Equating the coefficients of $r^0 t^{2k}$ from the both sides of (22) we get

$$b_{0,k+1} = \frac{1}{(k+1)(2k+1)}[140v^2 + \langle u^2\rangle c_k]. \quad \ldots (23)$$

Again substituting (14) in (21) we get

$$4\int_0^\infty \sum_{i=0}^\infty \sum_{k=1}^\infty \sum_{l=2}^\infty \sum_{m=o}^\infty l(l-1)(2l+3) b_{i,k} b_{l,m}\, r^{2i+2l-3} t^{2m+2k} dr = \sum_{k=0}^\infty c_k\, t^{2k}. \quad \ldots (24)$$

Equating the terms involving t^{2k} from the both sides of (24) we obtain

$$4\sum_{p=0}^k \int_0^\infty \sum_{i=0}^\infty \sum_{l=0}^\infty (l+1)(l+2)(2l+7)\; b_{i,k-p} b_{l+2,p}\, r^{2i+2l+1} dr = c_k. \quad (25)$$

3. Conclusions

The purpose of this paper is to present the possibility of solving the system of equations (4), (1), (6) and (7). If the condition (19) is fulfilled, the system of equations for $m_1(r, t)$ and $f(r, t)$ has the solutions in the class of functions expressed in power series (13) and (14) respectively. To determine these solutions it is necessary to know the coefficients $a_{i,0}$ and $b_{i,0}$ from experiment or another theory of homogeneous isotropic and stationary

turbulence, which considers Millionstchikov's hypothesis as fulfilled. It may be mentioned that this hypothesis of quasi normality sometimes leads to unphysical conditions and it may be applied only for short time intervals.

Our paper giving a formal solution to the system of equations (6) and (7) should arouse interest and attempts should be made to find the physical aspects of the results obtained and to verify them experimentally.

References

1. Panchev, S.– Random functions and turbulence, Pergamon Press, Oxford, (1971).
2. Von Karman, T. and Howarth, L. – On statistical theory of isotropic turbulence, Proc. Roy. Soc., Series A , 164 (1938).
3. Loitzianskii, L. G. – Some fundamental laws of isotropic turbulent flow, Trudy CAHI, No. 440 (1939).
4. Millionstchikov, M. D. – On the theory of homogeneous and isotropic turbulence, Dokl. Acad. Nauk SSSR, **32**, 615 (1941).
5. Chandrashekhar, S.– A theory of turbulence, Proc. Roy. Soc., **A229**, 1-19,(1955).
6. Chandrashekhar, S.– Theory of turbulence, Phys. Rev.,**102(4)**, 941, (1956).
7. Chandrashekhar, S.– The theory of turbulence, J. Madras Univ., **B27**(1), Centenary Number, 251(1957).
8. Jain, P. C.– Isotropic temperature fluctuations in isotropic turbulence, Proc. Nat. Inst. Sci. India, Vol. 28, A, No.3, 401-416 (1961).

INFORMATION TO AUTHORS

Manuscripts should represent results of original works on theoretical physics or experimental physics with theoretical background or on applied mathematics. Letters to the Editor and Review articles in emerging areas are also published. Submission of the manuscript will be deemed to imply that it has not been published previously and is not under consideration for publication elsewhere (either partly or wholly) and further that, if accepted, it will not be published elsewhere. It is the right of the Editorial Board to accept or to reject the paper after taking into consideration the opinions of the referees.

Manuscripts may be submitted in pdf/MS word format to **admin@citphy.org or susil_vcsarkar@yahoo.co.in** Online submission of the paper through our **website: www.citphy.org** is also accepted. The file should be prepared with 2.5 cm margin on all sides and a line spacing of 1.5.

The title of the paper should be short and self-explanatory. All the papers must have an abstract of not more than 200 words, the abstract page must not be a part of the main file. Abstract should be self-contained. It should be clear, concise and informative giving the scope of the research and significant results reported in the paper. Below the abstract four to six key words must be provided for indexing and infornjation retrieval.

The main file should be divided into sections (and sub-sections, if necessary) starting preferably with introduction and ending with conclusion. Displayed formula must be clearly typed (with symbols defmed) each on a separate /'ine and well-separated from the adjacent text. Equations should be numbered with on the right-hand side consecutively throughout the text. Figures and Tables with captions should be numbered in Arabic numerals in the order of occurrence in the text and these should be embedded at appropriate places in the text. Associated symbols must invariably follow SI practice.

References should be cited in the text by the Arabic numerals as superscript. All the references to the published papers should be numbered serially by Arabic numerals and given at the end of the paper. Each reference should include the author's name, title, abbreviated name of the journal, volume number, year of publication, page numbers, as in the simple citation given below :

For Periodicals : Sen, N.R. - On decay of energy spectrum of Isotopic Turbulence, 1. Appl. Phys. **28,** No. l0, l09-110 (1999).

1. Mikhilin, S. G. - Integral Equations, Pergamon Press, New York (1964).
2. Hinze, A. K. - Turbulence Study of Distributed Turbulent Boundary Layer Flow, Ph.D, Thesis, Rorke University (1970).

The corresponding author will receive page proof, typically as a pdf file. The proof should be checked carefully and returned to the editorial office within two or three days. Corrections to the proof should be restricted to printing errors and made according to standard practice. At this stage any modifications (if any) made in the text should be highlighted.

To support the cost of publication of the journal, the authors (or their Institutions) are requested to pay publication charge Rs.200/- per printed page for authors of Indian Institutes and US$ 20 for others. Publication charges to be sent directly to **CALCUTTA INSTITUTE OF THEORETICAL PHYSICS, 'BIGNAN KUTIR', 4/1, MOHAN BAGAN LANE, KOLKATA-700 004, INDIA.**

A pdf of the final publisher's version of the paper will be sent to the corresponding author shortly after print publication by our Co-publisher, **Wilcox Books & Periodicals Co. (wilcoxbooks@gmail.com)**

All communications are to be sent to the Secretary, Calcutta Institute of Theoretical Physics, 'Bignan Kutir', 4/1, Mohan Bagan Lane, Kolkata-700 004.

Indian Journal of Theoretical Physics is in the list of Journals approved by UGC.

For details please visit our website www.citphy.org

PUBLICATIONS
OF
CALCUTTA INSTITUTE OF THEORETICAL PHYSICS

"BIGNAN KUTIR"
4/1, Mohan Bagan Lane, Kolkata - 700 004, India
Phone: +91-33-25555726

INDIAN JOURNAL OF THEORETICAL PHYSICS (lSSN : 0019-5693)

Research Journal containing Original Papers, Review Articles and Letters to the Editor is published quarterly in March, June, September and December and circulated all over the world.

Subscription Rates

₹ 1500 per volume (for Bonafide Indian Party)
US $ 350 (for Foreign Party)

Back Volume Rates

₹ 1500 per volume (for Bonafide Indian Party)
US $ 350 per volume or Equivalent Pounds per volume

Books Written by Prof. K. C. Kar, D. Sc.

- **INTRODUCTION TO THEORETICAL PHYSICS**
  [Vol. I and Vol. II (Accoustics)]
  Useful to students of higher physics
  Price : ₹ 60 or US $ 10 per volume
- **WAVE STATISTICS : Its principles and Applications**
  [Vol. I and Vol. II]
  Useful to Post Graduate and Research students
  Price : ₹ 80 or US $ 12
- **STATISTICAL MECHANICS : Principles and applications**
  [Vol. I and Vol. II]
  Useful to Advanced students of Theoretical Physics
  Price : ₹ 120 or US $ 15
- **A NEW APPROACH TO THE THEORY OF RELATIVITY**
  Useful to post Graduate and Advanced students
  Price : ₹ 50 or US $ 8

Order may be sent directly to Calcutta Institute of Theoretical Physics
"Bignan Kutir", 4/1, Mohan Bagan Lane, Kolkata -700 004, India

---

Unimage, 10, Roy Bagan Street, Kolkata-700 006 and published by Dr. S. K. Sarkar, Secretary, on behalf of Calcutta Institute of Theoretical Physics, 4/1, Mohan Bagan Lane, Kolkatta -700 004, India.

Detailed information about our other Journals

1. Name of the Journal : **Bengal Past & Present**
   ISSN :..... **0005-8807**
   Frequency:..... **Annually (Latest Vol. 136,2017)**
   Price: .....(a) In India: Institutions: **500-00**
   .....(b) Overseas : **$ 150-00**
   Postage:..... **Post Free**
   * Discount :.... To Subscription Agencies: **25%**
   ..... To Institutions :..... **Fixed Price**
2. Name of the Journal:..... **Journal of the Indian Anthropological Society**
   ISSN :..... **0019-4387**
   Frequency:..... **Three Issues in a year (March, July & November)**
   Price:..... (a) In India: Institutions: **1500-00 (Latest Vol. 51, 2016)**
   ..... (b) Overseas..... **$ 300-00**
   Postage:..... **Post Free**
   * Discount: To Subscription Agencies: **25%**
   ..... To Institutions :..... **Fixed Price**
3. Name of the Journal: ..... **Journal of Surface Science and Technology**
   ISSN :..... **0970-1893**
   Frequency:..... **Quarterly**
   Price:..... (a) In India: Institutions: **1800-00 (Latest Vol. 33, 2017)**
   ..... (b) Overseas..... **$ 300-00**
   Postage :.....**Post Free**
   * Discount: To Subscription Agencies: **25%**
   ..... To Institutions :..... **Fixed Price**
4. Name of the Journal: **The Journal of the Indian Academy of Philosophy**
   ISSN: .....
   Frequency:..... **Bi-Annual**
   Price:..... (a) In India: Institutions: **200-00 (Latest Vol. 52, 2013)**
   ..... (b) Overseas..... **$ 30-00**
   Postage :..... **Post Free**
   * Discount :... To Subscription Agencies: **25%**
   ..... To Institutions :..... Fixed Price
5. Name of the Journal: **The Quarterly Review of Historical Studies**
   ISSN:..... 0033-5800
   Frequency:..... **Quarterly**
   Price:..... (a) In India: Institutions: **1500-00 (Latest Vol. 57, 2017-18)**
   ..... (b) Overseas..... **$ 400-00**
   Postage:..... **Post Free**
   * Discount :... To Subscription Agencies: **25%**
   ..... To Institutions: **Fixed Price**
6. Name of the Journal: **Indo-Iranica**
   ISSN:.....03789-0856
   Frequency:..... **Quarterly**
   Price:..... (a) In India: Institutions: **1500-00 (Latest Vol. 69, 2016)**
   ..... (b) Overseas..... **$ 350-00**
   Postage:.....**Post Free**
   * Discount : To Subscription Agencies: **25%**
   ..... To Institutions :..... **Fixed Price**

For more Journals Visit our website : www.wilcoxjournals.com

*** For Foreign Subscriptions Only**

Order should be sent to :

Wilcox Books and Periodicals Co.
8/2/A, Neogi Para Road,
Kolkata - 700036 (India)
Email : wilcoxbooks@gmail.com
: wilcoxbooks@yahoo.co.in